Thesis

Clinical value of semi-quantitative parameters “tumor-to-brain ratio” (TBR) in ^{18}F-FET PET/CT in the assessment of recurrence of gliomas in a single-center retrospective analysis

submitted by

Meilikhov Georgii

in partial fulfillment of the requirements for the degree of

Doktor der gesamten Heilkunde

(Dr. med. univ.)

at the

Medical University of Graz

executed at the

Department of Radiology
Division of Nuclear Medicine

under the supervision of

Univ.-Ass. Dr. Friedrich Weitzer

Dr. Birgit Pernthaler

Univ.-Prof. Dr. Reingard Maria Aigner

Graz, 06 May 2025

Declaration of Academic Integrity

I hereby confirm that the present diploma thesis is the result of my own independent scholarly work. I also confirm that in all cases where material from the work of others (in books, articles, essays, dissertations, and on the internet) is acknowledged, quotations and paraphrases are clearly indicated. No material other than that cited in the reference list has been used. I have read and understood the Medical University's regulations and procedures concerning plagiarism.

Furthermore, I hereby declare that if artificial intelligence (AI) tools were used for the generation, translation and/or correction of certain text passages in the creation of this work, such employment was conducted in compliance with ethical principles, academic integrity, and the regulations of my university. Additionally, it was ensured that this usage was transparently disclosed and appropriately attributed.

Graz, 06 May 2025 Meilikhov Georgii m.p.

Zusammenfassung

Titel: Wertigkeit der Tumor-to-Brain Ratio (TBR) in der ^{18}F-FET PET/CT bei der Rezidivbeurteilung von Gliomen in einer retrospektiven Analyse

Hintergrund: Gliome sind eine heterogene Gruppe von neuroepithelialen Tumoren mit vielen klinischen Erscheinungsformen und mit oft, je nach molekularem Profil, schlechter Prognose. Ihre Diagnose und Behandlung erfordert interdisziplinäre Zusammenarbeit. Die Diagnostik wird dabei oft von bildgebenden Diagnoseverfahren geleitet. Obwohl in der Vergangenheit als zweitrangig gegenüber der MRT betrachtet, haben jüngste Fortschritte wie die PET-RANO-1.0-Leitlinien die molekulare Bildgebung zur Bewertung des Tumoransprechens und therapeutischen Entscheidungen in den Vordergrund gestellt. Standardisierte Scan-Protokolle ermöglichen ein differenzierteres Verständnis des Tumorverhaltens.

Ziel dieser retrospektiven Studie war die Evaluierung der Wertigkeit semiquantitativer Parameter in der ^{18}F-FET PET/CT Untersuchung zu zwei Untersuchungszeitpunkten bei PatientInnen bei histologisch gesicherten Gliomen mit Rezidivverdacht.

PatientInnen und Methoden: Auf der Klinischen Abteilung für Nuklearmedizin wurden 198 PatientInnen mittels ^{18}F-FET PET/CT mit Gliomen untersucht und insgesamt 218 PET/CT-Scans durchgeführt. Das finale PatientInnenkollektiv umfasste 16 PatientInnen, bei denen ein histologisch bestätigter und/oder radiologisch hochverdächtiger Rezidivverdacht bestand und die sich mindestens zwei Scans unterzogen. Die dynamische Akquisition mit ^{18}F-FET wurde über 40 Minuten direkt nach i.v. Injektion des Radiopharmakons durchgeführt. In der retrospektiven Bildanalyse wurden die TBRmax und die TBRmean in der frühen Phase (10 Minuten p.i.) und in der späten Phase (20-40 Minuten p.i.) ausgewertet.

Zur Unterscheidung zwischen suspizierten Rezidiv und Therapie assoziierten Veränderungen wurde ein Cut-off der TBRmax von 1.6 herangezogen. Darüber hinaus wurde die Interobserver-Variabilität zweier Nuklearmediziner bei der visuellen Beurteilung von ^{18}F-FET-PET/CT in der Rezidiv Diagnostik untersucht.

Ergebnisse: Die TBRmax stieg in der späten Phase um 15% an (TBRmax, 2.79 ± 1.31 vs 2.87 ± 1.07), während die TBRmean tendenziell um 13% sank (TBRmean, 2.39 ± 0.98 vs 2.18 ± 0.72). Die TBRmean in der frühen Phase zeigte eine moderate Korrelation (R Spearmen=0.4092; p-value=0.018) mit dem WHO-Grad des Tumors.

In 12/35 Fällen (34%) wurden die PatientInnen aufgrund der ^{18}F-FET PET/CT Ergebnisse mit Verdacht auf ein Rezidiv einer erneuten Operation oder/und Bestrahlung unterzogen. Die statistische Analyse ergab jedoch keinen signifikanten Zusammenhang zwischen positiven Scans und therapeutischen Entscheidungen.

Gemäß der semiquantitativen Analyse der ^{18}F-FET-PET/CT wurden vier Fälle als Tumorrezidiv (TR) interpretiert, welche in der MRT als behandlungsbedingten Veränderungen (TRC) eingestuft wurden. Die Auswertung der frühen Phase ergab einen medianen SUVmax-Wert von 4.56±3.48 und einen medianen SUVmean von 2.50±1.9; in der späten Phase einen medianen SUVmax- und SUVmean von 6.50±3.93 bzw. 3.14±2.30.

Die Interobserver- Analyse zweier Nuklearmediziner zu subjektiver Bewertung der ^{18}F-FET PET/CT lieferte idente Ergebnisse.

Schlussfolgerung:

Die ^{18}F-FET PET/CT stellt ein innovatives, präzises nuklearmedizinisches Diagnoseverfahren zur Erstdiagnose sowie zur Evaluation der Therapie von Gliomen dar.

Das Ziel der retrospektiven Studie war die Wertigkeit der semiquantitativen Parameter zu zwei Untersuchungszeitpunkten bei PatientInnen mit histologisch verifizierten Gliomen und Verdacht auf Rezidiv zu bewerten. Es zeigten sich keine signifikanten Unterschiede der Messparameter in den unterschiedlichen Untersuchungsphasen. Ein statistisch belegter mäßiger Zusammenhang zwischen TBRmean in der frühen Phase und WHO-Tumorgrad war nachweisbar. Das Fehlen von Gliomen des Grades 3 schmälert jedoch die Gültigkeit dieser Beobachtung.

Das Verfahren gewährleistet eine metabole Differenzierung von behandlungsbedingten Veränderungen (treatment related changes) und Rezidiv Gliomas (tumor reccurence) und ist damit ein wichtiger Bestandteil für die weitere Therapieplanung.

Die Interobserver-Analyse ergab eine signifikante statistische Übereinstimmung bei der visuellen Bildinterpretation bei Gliom/Rezidivverdacht.

Prospektiv sollte die standardisierte visuelle Bildinterpretation etabliert werden. Zusätzlich sollte die Rolle der semiquantitativen Parameter mit Berücksichtigung der quantifizierenden Parameter, davon insbesondere time-to-peak, in größeren Studien evaluiert werden.

Abstract

Title: Clinical value of semi-quantitative parameters “tumor-to-brain ratio” in ^{18}F-FET PET/CT in the assessment of recurrence of gliomas in a single-center retrospective analysis

Background: Gliomas are a heterogeneous group of neuroepithelial tumors with many clinical manifestations and often with poor prognosis, which depends on molecular profile. Their diagnosis and treatment require a deep approach in an interdisciplinary team. Usually, medical treatment is guided by diagnostic imaging techniques. Although considered secondary to MRI in the past, recent advances such as the PET-RANO 1.0 guidelines for assessing response to tumor treatment have made nuclear medicine imaging a critical part of therapeutic decision-making. These standardized scan protocols allow for a more nuanced understanding of tumor behavior.

The aim of this retrospective study was to evaluate the value of semi-quantitative parameters in ^{18}F-FET PET/CT at two time points in patients with histologically confirmed gliomas suspected of recurrence.

Patients and Methods: One hundred and ninety-eight patients with glioma were examined by ^{18}F-FET PET/CT, and a total of 218 PET/CT scans were performed at our Clinical Division of Nuclear Medicine. The final patient collective included 16 patients with 35 scans with histopathologically confirmed gliomas and/or radiologically highly suspicious recurrence of tumors. These patients underwent at least two studies. Dynamic acquisition with ^{18}F-FET PET/CT was performed over 40 minutes directly after i.v. injection of the radiopharmaceutical. In the retrospective image analysis, the TBRmax and TBRmean were evaluated at 10 minutes and 20-40 minutes.

A TBRmax cut-off 1.6 was implemented to differentiate between suspected recurrence and treatment-related changes. Furthermore, the interobserver variability of two nuclear medicine physicians in the visual assessment of ^{18}F-FET PET/CT for recurrence diagnostics was examined.

Results: In the analysis, TBRmax increased by 15% in the late phase (TBRmax, 2.79 ± 1.31 vs 2.87 ± 1.07), while TBRmean tended to decrease by 13% (TBRmean, 2.39 ± 0.98 vs 2.18 ± 0.72). TBRmean at the early phase showed a moderate correlation (R Spearmen=0.4092; p-value=0.018) with the WHO grade of the tumor.

In 12/35 cases (34%), patients underwent reoperation and/or reirradiation based on the ^{18}F-FET PET/CT results with suspected recurrence. However, the statistical analysis showed no statistically significant correlation between positive scans and therapeutic decisions.

Four cases were interpreted as tumor recurrence (TR) according to the semi-quantitative analysis of ^{18}F-FET PET/CT, as evaluated by MRI data showing treatment-related changes (TRC). Early dynamic acquisitions showed a median SUVmax value of 4.56±3.48 and a median SUVmean value of 2.50±1.9. At the late phase, SUVmax and SUVmean values reached 6.50±3.93 and 3.14±2.30, respectively.

The interobserver analysis of two nuclear medicine physicians on subjective evaluation of ^{18}F-FET PET/CT yielded identical results.

Conclusion: ^{18}F-FET PET/CT is a new, accurate nuclear medicine modality for initial diagnosis and treatment evaluation of gliomas.

This retrospective study aimed to evaluate the value of semi-quantitative parameters in the ^{18}F-FET PET/CT at two examination time points in patients with histologically confirmed gliomas and suspected recurrence. There were no significant differences in the calculated parameters at the different time points. Only a moderate correlation between values of the TBRmean in the early phase and the WHO grade was present. However, the absence of grade 3 gliomas makes this observation invalid.

This method provides excellent metabolic differentiation between treatment-related changes (TRC) and tumor recurrence (TR) of gliomas, a crucial component for treatment decisions.

The interobserver analysis showed high agreement for the image interpretation in suspected recurrence of glioma.

Standards of visual image interpretation should be prospectively established. The role of semi-quantitative parameters should also be researched in larger studies, where quantitative parameters such as time-to-peak should be considered.

Declaration of previous publications

I hereby declare that I have not published any form of scientific work before writing this thesis.

Inhaltsverzeichnis

1. Abbreviations and their explanations

CNS	central nervous system
VEGF	vascular endothelial factor
AED	anti-epileptic drug
MRI	magnetic resonance imaging
RT	Radiation therapy
TMZ	temozolomide
Gy	Gray
WHO	World Health Organization
DNA	deoxyribonucleic acid
MGMT	methyltransferase
IDH	isocitrate-dehydrogenase
DWI	diffusion-weighted sequence
CT	computed tomography
TR	tumor recurrence
TRC	treatment-related changes
RANO	The Response Assessment in Neuro-oncology
MRS	magnetic resonance spectroscopy
PET	positron-emission tomography
keV	kilo electron volt
PMT	photomultiplier tubes
LOR	line of response
TOF	Time-of-Flight
SPECT	single photon emission computed tomography
SUV	standardized uptake values
AC	attenuation correction
ROI	region of interest
VOI	volume of interest
^{18}F-FET	O-(2-[18F]-fluoroethyl)-L-tyrosine
^{11}C-MET	^{11}C-methionine
LAT1	large amino acid transporter type 1
^{18}F-FDG	[^{18}F]-2-fluoro-2-deoxy-D-glucose
GLUT	glucose transporter

TBR	Tumor-to-Brain ratio
FOV	field of view
BTV	biological tumor volume
EANM	European Association of Nuclear Medicine
EANO	European Association of Neuro-Oncology
MBq	Mega Becquerel
TTP	Time-to-peak
i.v.	intravenous
p.i.	post-injection

2. List of Figures

3. List of Tables

4. Introduction

4.1 Gliomas definition and epidemiology

Gliomas are a group of neuroepithelial tumors of the central nervous system (CNS) that develop from glia in the brain and the spinal cord. Therefore, gliomas histologically have features that are similar to normal glial cells (1), including their genetic profiles and morphology that can be viewed microscopically. Gliomas nomenclature is based on a variety of cellular origins. These tumors are one the most aggressive neoplasms with poor prognosis (2). Gliomas have an annual incidence of about 5-6 per 100,000 in German-speaking countries (3), 6 per 100,000 in the USA, and 3.19 per 100,000 worldwide (4,5).

While primary CNS tumors have an incidence of only 2% in all primary cancers, they are responsible for 7% of cancer-related deaths in individuals under the age of 70 (6). Most gliomas occur in one of the four lobes of the brain: the frontal lobe (23.6%), the temporal lobe (17.5%), the parietal lobe (10.4%), and the occipital lobe (2.6%). A minority of cases, however, manifest in the brainstem, cerebellum, and spinal cord (5).

The incidence of primary CNS tumors is higher in white individuals than in other racial groups (7). The incidence of gliomas varies according to the specific type. Pilocytic astrocytomas are more common in children and adolescents, while low-grade diffuse oligodendrogliomas usually affect patients under 50 years of age with a peak incidence between 30 and 40 years of age (8). The most frequent malignant primary brain tumor in adults is glioblastoma, which increases after 40 years of age, with a peak incidence in the age group of 55-84 (5,8).

	WHO grade	**Histology**	**%**	**Characteristics**	**Estimated 5-year survival (%)**
Benign		Ependymoma: subependymoma, subependymal giant-cell astrocytoma	5.2	Can be slow or fast growing Usually located in ventricles Common in children	65
Low grade	1	Pilocytic astrocytoma, also known as Juvenile Pilocytic Astrocytoma	5.1	Slow growing, usually benign, often cystic Most common in the cerebrum Occurs most often in children and teens	98

	WHO grade	Histology	%	Characteristics	Estimated 5-year survival (%)
	2	Oligodendroglioma (5%)	28.0	Tend to be slow growing Rarely grow outside of brain	50
		Astrocytoma (17.4%)			
		Oligoastrocytoma (5.6%)			
High grade	3	Anaplastic astrocytoma	6.7	Grows faster and more aggressively than grade II Tend to invade neighboring tissue	30
		Anaplastic oligodendroglioma			
		Anaplastic oligoastrocytoma			
	4	Glioblastoma	55.0	Can develop directly (de novo) or evolve from low-grade tumor Highly invasive in brain	<5

Table 1: Characteristics and statistics related to selected gliomas (9).

One of the few known risk factors that have been reported to increase the probability of developing gliomas significantly is ionizing radiation (10). Radiation-induced glioblastoma nearly always occurs years after therapeutic radiation was given for the treatment of another neoplastic or non-neoplastic condition (11). Other factors like electromagnetic fields, formaldehyde or non-ionizing radiation from cell phones have no evidence that they may be the cause of glioblastoma development (12). However, specific genetic diseases such as neurofibromatosis types 1 and 2, tuberous sclerosis, Li-Fraumeni syndrome, and Turcot syndrome may be associated with an increased predisposition to glioma development (13,14). However, fewer than one percent of all patients with diagnosed gliomas has an identifiable hereditary disorder (10).

Newly diagnosed gliomas can be presented clinically differently, depending on tumor size, location, and the extent of involvement of brain structures. The most common symptoms are:

- Headaches: this can be present in up to 50% of cases (15).
- Nausea and vomiting are quite common symptoms: These will most commonly occur due to tumor growth and increased intracranial pressure.
- Focal neurological signs: Presentation is variable and is based on the tumor's location.

- Cranial neuropathies: ocular palsies, deafness, or dysphagia can occur due to leptomeningeal dissemination or intracranial hypertension.
- Papilledema: This can be found during a physical examination and can be interpreted as a sign of intracranial hypertension.
- Cognitive and Personality Changes: Frontal lobe dysfunction (16) can lead to irritability, aggression, apathy or loss of initiative, indifference, egocentrism, decreased empathy, loss of emotional control, and disinhibition.
- Episodic loss of consciousness (plateau waves): can mimic seizures (17).
- Seizures are present in 74% of the patients (18).

4.2 Treatment

The treatment of newly diagnosed gliomas requires a multimodal and interdisciplinary approach. The three main pillars are:

- surgical treatment
- radiotherapy
- chemotherapy in the form of neoadjuvant chemotherapy.

A new treatment method, immunotherapy, is also being utilized. A commonly used immunotherapy drug is bevacizumab, a monoclonal antibody. Its action is based on the inhibition of vascular endothelial growth factor (VEGF). Glioblastoma is characterized by high vascularization due to increased synthesis of this factor. The use of bevacizumab may therefore improve prognosis (19).

Regarding clinical features, a prescription for anti-epileptic drugs (AEDs) may be written based on the features spotted by the clinician. Previously used drugs, such as AEDs like phenobarbital or phenytoin and carbamazepine, are not considered first-line therapies and can both induce hepatic cytochrome P450 and thus negative affect the metabolism. Therefore, the first choice of AEDs is non–enzyme inducing drugs like levetiracetam or clobazam are preferred because of the lack of drug interactions and better side effect profile (20). In addition, treatments against tumors may decrease further attack cycles (21).
Many patients receive corticosteroids at the initial diagnosis to help control vasogenic edema and relieve the signs and symptoms often associated with it (22). Dexamethasone is chosen over other options because of its low mineralocorticoid effect and long half-life. If severe

neurological features include gait or even level of consciousness disturbances, a bolus dose of 10 mg of dexamethasone can be given, followed by 16 mg per day (23).
Venous thromboembolism affects 10-30% of patients with gliomas (24) and has an increased risk in the postoperative period, direct. Patients who have undergone neurological surgery and receive prophylactic treatment with low molecular weight heparin or unfractionated heparin should begin treatment at least 24 hours after the completion of surgery (25).

4.2.a. Surgical treatment

Maximum surgical resection of tumor tissue with minimal excision of healthy tissue is the best treatment option. Considering the fact that gliomas are often characterized by invasive growth and may be located in areas of the brain with critical structures, such as speech, motor or subcortical centers, performing such surgeries can be difficult. Thus, the chances that tumor cells may remain in the tissue after surgery are high. Preoperative mapping techniques, such as neuronavigation, allow for the broadest possible resection of tumors and avoid perioperative damage to critical brain structures. This preserves normal function and quality of life (26). Preoperative mapping techniques also include conventional magnetic resonance imaging (MRI), functional MRI, and diffusion-tensor imaging. They play an important role in minimizing the occurrence of unwanted neurological deficits after surgery and, consequently, disabilities (27).

Though significant surgical improvement has been achieved in the resection of gliomas, the overall survival rate is still poor. At this point, the prognosis for low-grade gliomas remains relatively good with a median survival of five years. For high-grade gliomas, including astrocytomas, oligoastrocytomas, and oligodendrogliomas, survival is less than five years. Median survival for glioblastomas is as close to fifteen months (28).

Tumors reaching 5-6 cm in diameter and also crossing the midline are associated with unfavorable outcomes (10). Regarding lesion localization, supratentorial (brain) and cerebellar lesions are better treated by surgery with a better prognosis than brainstem or diencephalic tumors (29).

4.2.b. Chemoradiation

Postoperative external beam radiation therapy (RT) together in combination with temozolomide (TMZ) chemotherapy remains the standard treatment for gliomas. Field RT is currently favored over whole-brain RT because the second method causes significant damage to normal brain tissue. The latter has been associated with a variety of substantial effects on late-onset, including endocrinopathy, neurocognitive toxicity, and radiation leukoencephalopathy (30). Thus, chemoradiotherapy prolongs the overall survival compared with chemotherapy or RT alone (31). A three-dimensional conformal beam RT is nowadays the standard-care. Still, the fast-developing intensity-modulated RT is taking more place in clinical practice because it optimizes the conformity of irradiation of irregular-shaped tumors, which is typical for gliomas, reducing the overall toxicity to healthy brain tissues (32). As it has been established that postoperative RT doses above 60 Gy can provide survival benefits, anything beyond 60 Gy is categorized into a high-risk category since it increases toxicity without enhancing overall survival (33).

4.3 Classification

The term “glioma” covers a whole group of tumors. In the past, malignant gliomas were classified into categories according to their histopathologic and phenotypic features. However, in the latest WHO classification of CNS tumors, newly discovered molecular characteristics along with previously known molecular characteristics have replaced several tumor categories and have increased the use of molecular analysis in diagnosis and grading. The last revision of the above elements was done in 2021. According to the 2007 WHO classification, gliomas were classified by their cell of origin, namely, astrocytic, and glial, oligodendroglial, mixed oligoastrocytial, ependymal, and neuronal and mixed neuronal-glial tumors (34). Current molecular biomarkers are more critical than the phenotype gliomas as supplementary or definitive diagnostic information. New tumor types are adult-type diffuse gliomas, pediatric-type diffuse low- and high-grade gliomas, circumscribed astrocytic gliomas, and gangliogliomas. These categories are further divided into subtypes depending on their molecular characteristics and histopathological profiles (35).

One of the crucial components of this and the prior WHO classifications is the CNS grading criteria that reflect the degree of tumor proliferation, touching upon parameters such as the

mitotic rate, the lack or presence of necrotic areas, and microvascular proliferation (17,36). It is expected that the system could relate the tumor grade to an ideal clinical, biological behavior, which will inform prognostic probabilities or courses if the disease is untreated. This system is designed to make it possible to diagnose a disease accurately, make dependable predictions of the course of sickness, and choose the best form of treatment for a specific disease.

As per this system, CNS WHO grade 1 tumors are slowly growing, and examples are diffuse astrocytoma and oligodendroglioma, which can be cured in most instances through surgery alone. On the other hand, CNS WHO grade 4 tumors like glioblastoma IDH-wildtype are lethal and invasive for which established treatment interventions are mandatory (37,38). These tumors are usually described by infiltrative growth patterns and a tendency to recur, even when the multidisciplinary protocol of treatment is applied, including maximal safe surgery, radiochemotherapy, and adjuvant systemic therapy (39).

The traditional method of grouping and ranking gliomas has been underperforming for several years, resulting in significant differences in survival rates among those diagnosed with gliomas. Clinical factors such as patient age, performance status, and resection volume are known to influence survival to some extent, its statistical differences suggest that some biology of tumors seems to have been overlooked. Recent improvements in the knowledge of molecular signatures within gliomas have expanded current diagnostic, prognostic, and therapeutic models for glioma classification and treatment (1).

Certain factors, molecular elements, mutations, or abnormalities in the tumor tissue can help characterize a tumor subtype or profile. It is possible to mention that identifying specific gene mutations is a valuable approach to distinguishing cases of high-grade tumors from low-grade ones. Polymorphisms of genes associated with drug metabolism affect therapeutical decisions (40).

The O6-methylguanine-DNA methyltransferase (MGMT) is an acknowledged protein-coding gene that encodes a DNA repair enzyme. The MGMT gene methylation makes it inactive; thereby, methylated MGMT genes exhibit poor DNA repair capability (41). This gene´s activity level correlates inversely proportional to the efficiency of alkylating antineoplastic agents such as TMZ. The mutation of the MGMT promoter is observed in 35 to 45% of high-grade gliomas and in about 80% of low-grade gliomas (42). It has been

proven that methylation of MGMT is a reliable biomarker for better prognosis in patients who are treated with TMZ (43). It has been found that mutations of isocitrate-dehydrogenase (IDH)-1 coding genes are present in 70% of grade 2-3 infiltrating gliomas (44).

The current molecular grading of oligodendrogliomas is based on the IDH mutation and 1p/19q codeletion. The latter is associated with a better prognosis (45). Diffuse astrocytomas are subcategorized into two groups: Those with mutated IDH, categorized as having an intermediate prognosis, and those without mutated IDH, wild-type, affiliated with poor prognosis. Some clinical trials have assessed the outcomes concerning molecular classification, and it has been postulated that using this type of classification might provide a better prognosis than if the conventional WHO grade of 1–4 is used.

World Health Organization Classification of Tumors of the Central Nervous System, fifth edition	
Gliomas, glioneuronal tumors, and neuronal tumors	
	• Adult-type diffuse gliomas • Pediatric-type diffuse low-grade gliomas • Pediatric-type diffuse high-grade gliomas • Circumscribed astrocytic gliomas • Glioneuronal and neuronal tumors • Ependymal tumors
Choroid plexus tumors	
Embryonal tumors	• Medulloblastoma • Other CNS embryonal tumors
Pineal tumors	
Cranial and paraspinal nerve tumors	
Meningiomas	
Mesenchymal, non-meningothelial tumors	
Melanocytic tumors	
Hematolymphoid tumors	• CNS lymphomas

	• Histiocytic tumors
Germ cell tumors	
Tumors of the sellar region	
Metastases to the CNS	

Table 2: 2021 WHO Classification of tumors of the CNS (35).

4.4 Imaging diagnostic of gliomas

Computed tomography (CT) and MRI play an essential role in the early diagnosis of gliomas, along with assessing their location, nature, size, and extent, which are vital in staging and setting up management strategies.

4.4.a. Magnetic resonance imaging

MRI is regarded as the best technique for diagnosing gliomas. As many patients with gliomas necessitate not only frequent but also detailed MRI scans to evaluate the effectiveness of the therapy, MRI is the most preferable type of imaging in this case. MRI provides better soft tissue contrast than other imaging techniques to help evaluate glioblastomas and characterize them due to the high sensitivity of MRI. It is a reliable way to determine whether a tumor is present, the extent of its invasion beyond the apparent borders due to its infiltrative nature, and whether there is peritumoral edema.

MRI with gadolinium contrast shows enhancement in glioblastomas. The most common observation is irregularly formed masses with a peripherally enhancing “halo” and a central area of non-enhancing necrosis. Thus, necrosis is considered the hallmark of malignant gliomas (36).

In about 13 % of cases, the tumor becomes multifocal (with more than two lesions, including leptomeningeal dissemination) or distant with a second lesion not anatomically related to the first, or the tumor becomes diffused. This finding is supported by data showing that intraoperative tumor invasion usually extends beyond the areas of altered signal seen on MRI (12,46). Another revolutionary improvement in neuroimaging is represented by MRI diffusion-weighted sequences (DWI) as the non-invasive assessment of cell density and the nature of gliomas (47). This development superseded computed tomography (CT) and has changed glioblastoma diagnostic strategy.

Even though a definitive diagnosis of glioblastoma depends on histopathology and genetic testing, structural MRI scans are typically used for pre-surgical staging.

MRI utilizing a variety of sequences, including T1, T2, and gadolinium-enhanced, is a vital diagnostic, characterization, follow-up, and evaluation tool for gliomas. MRI gives nicely defined structural pictures that reveal where a tumor is located and how wide an extension. That information can assist with the diagnosis process. However, one of the principal drawbacks of conventional MRI is that the procedure is not biology-specific to tumors. For example, T2-weighted signals predominantly come from tissue water content, and contrast enhancement is a result of enhanced blood-brain barrier permeability. These make it challenging the diagnosis and characterization of gliomas without invasive procedures.

Standard MRI is a reliable diagnostic method, because it provides important anatomical information and is widely available worldwide. However, it has no specific disease markers and advanced image processing options, restricting its diagnostic and prognostic value. Still, it is difficult to differentiate tumor recurrence (TR) from treatment-related changes (TRC), and there is an additional disadvantage related to the variety and specificity of histologic changes in gliomas that radiologists are unable to detect (48). The Response Assessment in Neuro-Oncology (RANO) criteria rely on linear measurements in only the enhancing tumor components, which do not reflect the complex morphology and heterogeneous nature of gliomas and, therefore, show low levels of concordance with prognosis factors.

The 2021 update to the WHO Classification has introduced further layers of complexity in the interpretation of contrast-enhanced tumor imaging, as the enhancement does not always correlate with malignancy grade. This makes it even more difficult to distinguish whether a tumor exists without a biopsy (49). Stereotactic biopsy is the reference method for differentiating TRC and TR, but its invasive nature restricts the daily practice.

Recently, advanced imaging techniques, including diffusion MRI, perfusion MRI, magnetic resonance spectroscopy (MRS), and positron emission tomography (PET), have been developed as non-invasive and feasible early TR and TRC identification methods. These techniques have consequently become key areas of research (50).

4.4.b. Computed tomography

CT is a useful diagnostic method, which is characterized by short scanning times, but also has several drawbacks in the detection of brain lesions. In the first place, CT has significantly lower spatial resolution and soft tissue contrast than MRI. Second, it exposes patients to relatively higher levels of ionizing radiation, resulting in dose accumulation that can deteriorate their health. Nevertheless, contrast-enhance CT has proved to be a major milestone in neuroradiology because it facilitates accurate anatomic localization of intracranial tumors, particularly malignant ones, because of the enhanced contrast feature (51).

In addition to CT and MRI, PET or PET/CT scans are other imaging methods used to diagnose gliomas.

4.4.c. Nuclear medicine imaging

4.4.c.1 **Positron emission tomography fundamentals**

Molecular imaging has recently gained increased importance in the primary diagnosis of CNS tumors and follow-up studies, in addition to routine diagnostic modalities such as CT and MRI.

PET is a functional imaging method that detects and allows the measurement of physiological and pathophysiological metabolism in vivo, blood flow, chemical composition, and absorption. Nuclear medicine imaging significantly offers clinicians useful molecular information about their patients (52).

The high value of molecular imaging lies in the ability to categorize tumor grade when a biopsy is not possible or gives false negative results, as well as in the prediction of genotype relevant for the correct treatment tactics; also, in re-staging studies, it allows differentiation of TRC from TR and making correct clinical decisions (48).

It is based on the detection of one form of ionizing radiation. The main principle is β^+ decay of isotopes, which produces the antiparticle of electron-positron that travels in tissue for a short distance (different by various isotopes) and then interacts with an electron in the body. This interaction is called an annihilation. With this annihilation, two gamma rays, i.e., high-energy photons, each with an energy of 511 keV, are emitted in opposite directions, i.e., at an angle of almost 180 degrees to each other, and are further detected by tomography

detectors. Scintillation crystals in detectors are usually made of sodium iodide (NaI), gadolinium oxyorthosilicate (GSO), or bismuth germanium oxide (BGO) and coupled with photomultiplier tubes (PMTs). The ring design of PET scanner detectors takes advantage of detecting two photons in close temporal proximity by two opposed detectors in the ring, which are likely to be from a single annihilation event; this simultaneous detection event is called coincidence.

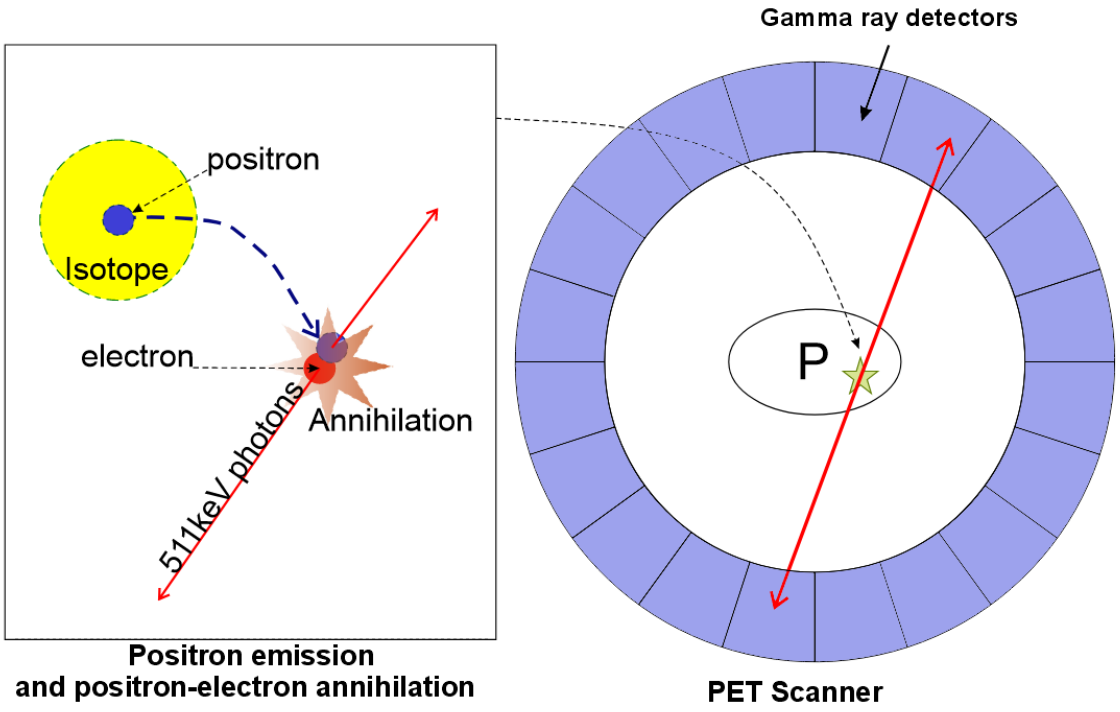

Figure 1: Basic physics of positron emission tomography (53). P: patient.

However, several challenges can affect the accuracy of coincidence and annihilation detection:

1. A positron travels only a short distance before the annihilation, and the mismatches between the time of emission and the time of the annihilation mean there is some uncertainty in identifying the location of the original positron emission.
2. Scattered coincidences: Depending on the interaction between one or both photons in body tissues, Compton scattering can alter the direction of the traveling photons, resulting in the wrong positioning of the annihilation event and distorting contrast images.
3. Random Coincidences: These arise when photons by different annihilation events are mistaken for being from the same pair, thus degrading the image by adding noise to the system. In this variant, a line of response (LOR) is located far from the actual event.

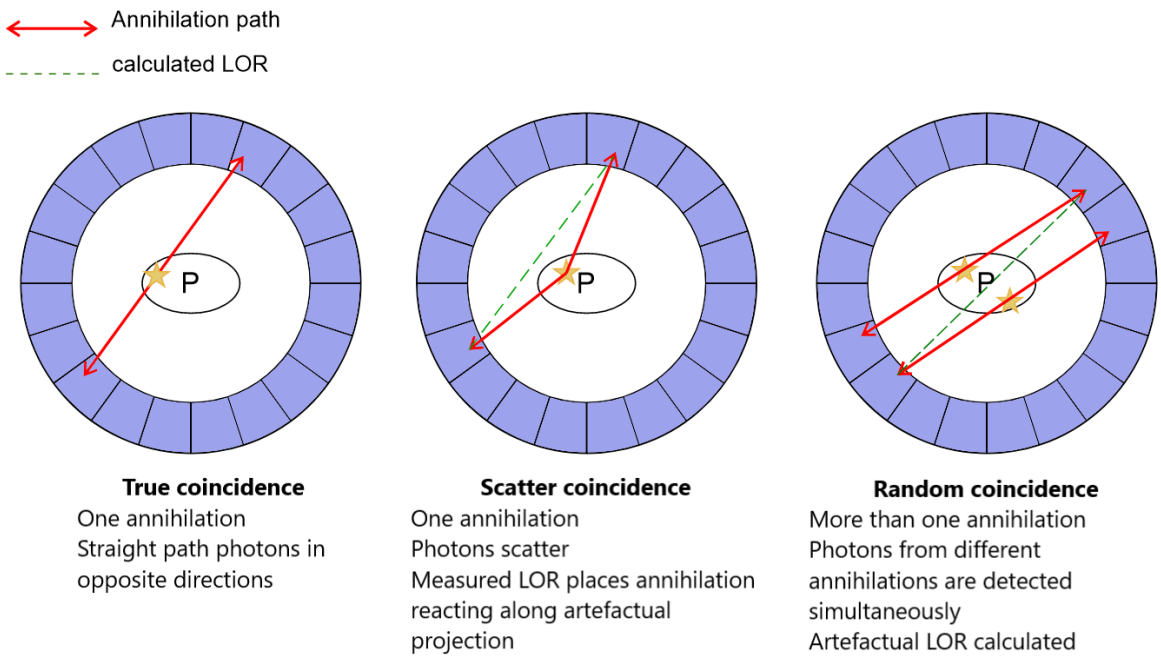

Figure 2: Types of unwanted coincidence. P: patient (54).

True events in PET imaging occur when both 511 keV photons from a positron annihilation are detected within the coincidence time window. These true coincidences provide accurate information for constructing PET images. To manage these issues, PET systems use timing precision to reduce random coincidences and energy windows to exclude scattered photons. However, this can also lead to the loss of some true events, balancing image quality with acquisition time. In the new generation of digital PET scanners, traditional PMTs have been replaced with semiconductor crystals, which transfer the scintillation impulses directly into electric pulses. In addition, the time-of-flight (TOF) technology that relies on the application of extremely fast gamma-ray detectors used in modern tomographs not only detects the distance and attenuation of the photons but also enhances the algorithmic process by adding the actual real by incorporating the actual time difference between the detection of photons from coincidence events. This enables a more precise identification of the distance from the annihilation event to the detector. This permits a more precise measurement of the distance between the annihilation event and the detector. This technology also improves significantly the time resolution to approximately 400-500 picoseconds (55). This higher precision allows a higher rate of true beta decay events to be counted, leading to more precise and more accurate imaging. Further, all coincidences are recorded by PET scanner and reconstructed to produce cross-sectional images.

In vivo, molecular visualization in nuclear medicine relies on the use of tracers or radiopharmaceuticals, which are chemical compounds formed of two distinct parts:

- positron-emitting radioisotope,
- targeting molecule (or ligand) that is enriched in specific organs or tissues.

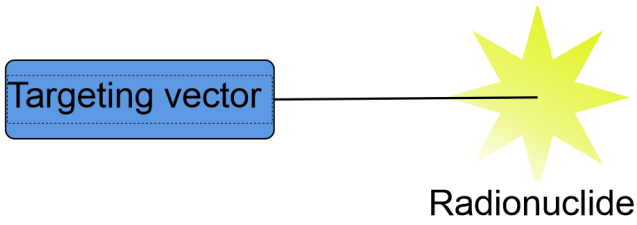

Figure 3: Principle of radiotracer.

Furthermore, the half-life time is very important as the synthesis, administration of tracers, and acquisition must be completed within a period compatible with the half-life (56). Some tracers are synthesized via cyclotron, including ^{11}C and ^{18}F. Other isotopes can be obtained through generator synthesis, for example, ^{68}Ga. Ligands could be peptides, specific antibodies, and some small molecules. There are also special molecules that are required to bind the isotope to the target molecule. These molecules are called chelators. For example, in ^{68}Ga-DOTA-TATE tracer, DOTA is the chelator or the linker.

Isotope	Production Method	Half-Life	Decay Mode(s)
^{11}C	Cyclotron	20.4 min	β^+ EC (0.21%)
^{13}N	Cyclotron	10 min	β^+
^{15}O	Cyclotron	2.03 min	β^+
^{18}F	Cyclotron	110 min	β^+ (97%) EC (3%)
^{68}Ga	Generator Cyclotron	68.3 min	β^+ (90%) EC (10%)
^{64}Cu	Reactor Cyclotron	12.7 hours	β^+ EC

Table 3: commonly used PET Radioisotopes. β^+: decay with positron emission, EC: electron capture (57,58).

However, achieving high-quality images with PET and single photon emission computed tomography (SPECT) can be difficult because of the noise in the measurement and the

occurrence of different types of artifacts. Over the past few decades, there have been rapid improvements in the hardware and software used in nuclear medicine, leading to increased image resolution and the introduction of molecular imaging for diagnosis. One of the most important advancements has been the development of hybrid scanners, which made it possible to integrate nuclear medicine with CT or MRI. Hybrid PET/CT and PET/MRI devices offer a unique chance to combine the functional imaging of PET with the high-resolution anatomical imaging of CT or MRI. In the case of a hybrid system PET/MRI, additional functional imaging gives an advantage and may have a significant impact on clinical treatment (59).

These developments have also been crucial in improving image reconstruction algorithms and thus improving the quality of the pictures in nuclear medicine. Anatomical information obtained from hybrid scanners has led to the design of sophisticated attenuation and scatter correction techniques (60,61) that have improved the quantitative and qualitative scans. These enhancements have increased the ability to diagnose diseases more accurately and achieve a better assessment of the tracer uptake, as depicted by the standardized uptake values (SUV).

Gamma rays from the injected positron-emitting tracers must travel through parts of the body before detection so that attenuation and scattering occur. Attenuation means a smaller number of 'true' coincidence events detected by the tomograph is reduced due to absorption or scattering outside the detector's field of view. This can be corrected using anatomical information during image reconstruction (62).

Measured attenuation correction (AC) involves actual transmission data from CT scans of the chest, abdomen, pelvis, and whole body that varies the attenuation. It provides an attenuation correction transmission map that can be calibrated to represent electron density, thereby allowing the AC to determine the effective differences in positron-emitting radionuclide absorption in different tissues. Indeed, PET/CT scanners can make it possible to perform rapidly generated attenuation maps within one breath-hold, and their quality is high. However, attenuation maps derived from computed tomography are obtained much faster than positron emission tomography itself, and artifacts in regions of moving structures such as the diaphragm may occur (63).

MRI AC provides information on proton density and MRI relaxation rates. However, MRI-based attenuation correction (MRAC) is still new, and this method has not been well accepted for clinical trials (64).

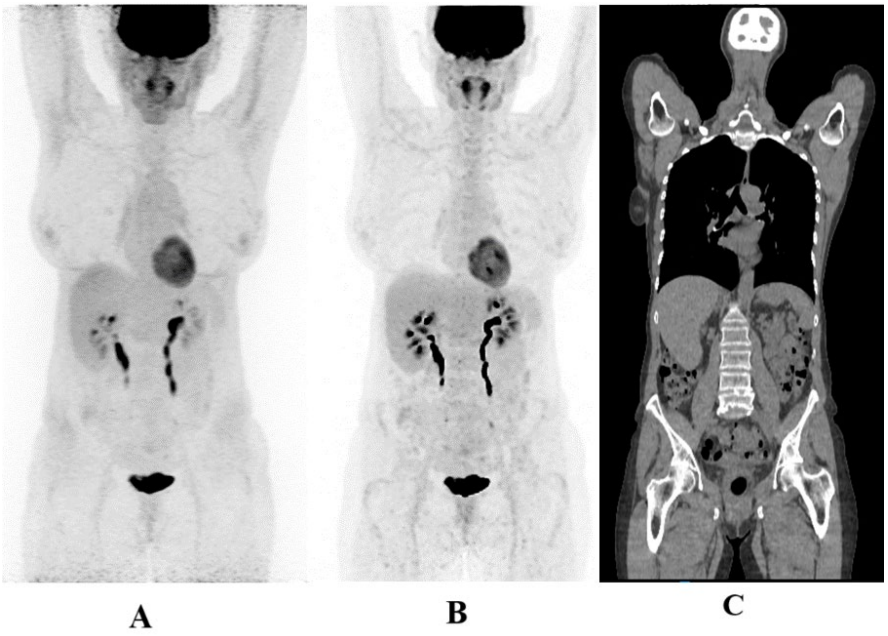

Figure 4: Attenuation correction basis. Images with no-AC ^{18}F-FDG PET scan (A), with AC (B) and corresponding CT (C). AC-images are characterized by lower skin tracer accumulation, low or absent uptake in lungs, which corresponds to air/small lung tissue density, and better visualization (no scatter effect) of adjacent tissues near the bladder and other organs that physiologically can accumulate specific radiopharmaceutical. The examination was performed in-house and showed no pathological distribution pattern.

4.4.c.2 **Quantitative analysis of PET images**

Another benefit of nuclear imaging is quantifying the number of radiotracers taken up by various tissues. In PET acquisitions, the most frequently applied index for assessing tracer uptake is the standardized uptake value (SUV). SUV is a semiquantitative index of the radioactivity concentration normalized to a patient's body weight in the PET images. The measured radioactivity within a region/volume of interest (ROI and VOI, respectively) is then standardized by the average activity concentration in the body, which is equal to the injected dose divided by the patient's body size. The body size measurements include body weight, lean body mass, and body surface area, with body weight being the most used in clinical practice. There are two common ways of reporting SUV: the mean or maximum SUV of all voxels within the VOI (SUV_{mean} and SUV_{max}, respectively). SUVmean contains information from several voxels and is less susceptible to image noise than SUVpeak.

However, the measured SUVmean will differ depending on which voxels are included within the average. Thus, it depends on the ROI definition and is intra- and inter-operator dependent (65). SUVmax is the maximum voxel activity within the ROI and hence is not reliant on ROI delineation (if the voxel with the maximum activity is included) but is more noise-sensitive (66). SUVmax is best measured by drawing a 3D VOI around the target lesion to ensure that a relatively large volume of interest is obtained without including the urinary bladder or other regions of high activity. Alternatively, 2D ROIs are visually placed on multiple axial slices with the highest radiopharmaceutical accumulation intensity to quantify the target's highest activity. Nowadays, SUVmax is most used because it does not depend on the observer to the same extent as SUVmean and can be reproduced more efficiently.

4.4.c.3 **Radiopharmaceuticals in PET diagnostics of gliomas**

In PET/CT glioma diagnostics, ^{11}C-methionine (^{11}C-MET) and O-(2-[18F]-fluoroethyl)-L-tyrosine (^{18}F-FET) are tracers that are being used nowadays. They are helpful in determining the intracellular transport of amino acids at the molecular level. The principle of tracers is based on hyperexpression of amino acid transport carriers via membranes such as large amino acid transporter 1 (LAT1) on the cell membrane. LAT1 is over-expressed in malignant tumors to cater to the needs of these fast-growing tumors (67,68). Also, the overexpressing of LAT1 correlates with poor prognosis and fulminant course of diseases (69,70). The bimolecular mechanism of these tracers is similar to [^{18}F]-2-fluoro-2-deoxy-D-glucose (^{18}F-FDG), which is used for imaging of cells with increased glucose metabolism. This depends on transmembrane transport by specific proteins, namely glucose transporter (GLUT1 and GLUT2). The amount of these proteins significantly increases in tumor cells. It is reported that amino acid-based tracers are superior to ^{18}F-FDG for drawing the margins of low-grade gliomas (71) because of high physiological glucose metabolism in brain tissue and the resulting decrease in the contrast between the potential lesion and healthy tissue.

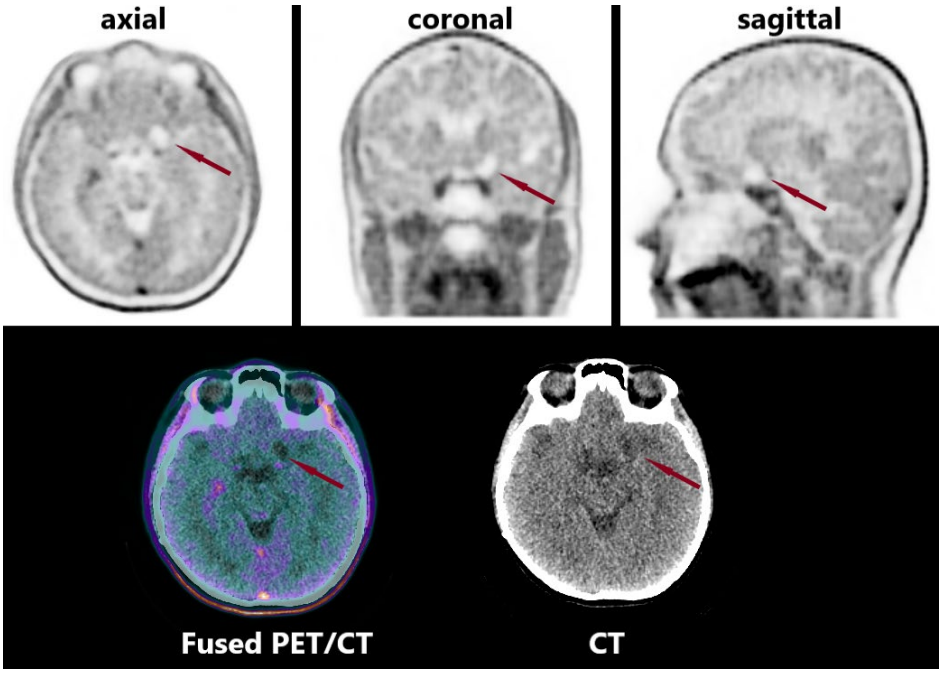

Figure 5: 40-year-old female patient with oligoastrocytoma WHO grade 4 after surgical treatment for twelve years and twelve cycles of adjuvant chemotherapy for five years. Diffuse, slightly physiological accumulation of ^{18}F-FET in gray matter, glandular structures, and venous vessels. A lack of tracer´s uptake frontobasal left in PET corresponds to a hypodense postoperative liquor-filled area on CT corresponding to the area of surgery (red arrows).

LAT1 has been viewed as the marker for predicting malignant changes and cell proliferation in high-grade gliomas. It has also been identified to be correlated with glioma angiogenesis (70). Nevertheless, 30 % of low-grade and 5% of high-grade gliomas do not demonstrate increased ^{18}F-FET uptake at diagnosis. In follow-up and disease progression, about 50 % of these ^{18}F-FET-negative gliomas with TBR<1.6 may convert to ^{18}F-FET-positive gliomas with TBR>1.6 (72).

^{11}C isotope is obtained in a cyclotron by the proton-bombardment ^{14}N target following ^{14}N (p, α)^{11}C nuclear reaction (58). However, due to a short half-life of 20.4 minutes, it is not economically practical for centers that do not have a cyclotron. In contrast, ^{18}F is also a positron-emitting radionuclide produced by irradiation with protons from a stable and naturally occurring isotope of oxygen-18 (^{18}O). With a half-life of 109 minutes, ^{18}F is more practical for use in nuclear medicine centers that do not have their own cyclotron.

A study by Katsanos et al. has revealed that ^{11}C-MET is more specific and sensitive than 18F-FET. However, this was not statistically significant (73). Another survey by Grosu et al. (74) showed that ^{18}F-FET PET and ^{11}C-MET PET provide comparable diagnostic information: sensitivity and specificity for tumor tissue are identical. Both ethyltyrosine (^{18}F-

FET) and methyltyrosine (^{11}C-MET) are taken up by glioma cells, providing good contrast with benign brain tissue as amino acid tracers. The accumulation of ^{18}F-FET is due to asymmetric recognition of the amino acid derivative on both sides of the cell membrane. This results in a capture mechanism without incorporation into proteins or metabolism (75).

A key advantage of ^{18}F-FET PET/CT is the possibility of quantitative analysis, especially with the Tumor-to-Brain Ratio (TBR). TBR provides an objective way to evaluate pathological FET uptake and represents the ratio of the maximum or mean standardized uptake volume in the tumor area to the mean standardized uptake in normal brain tissue.

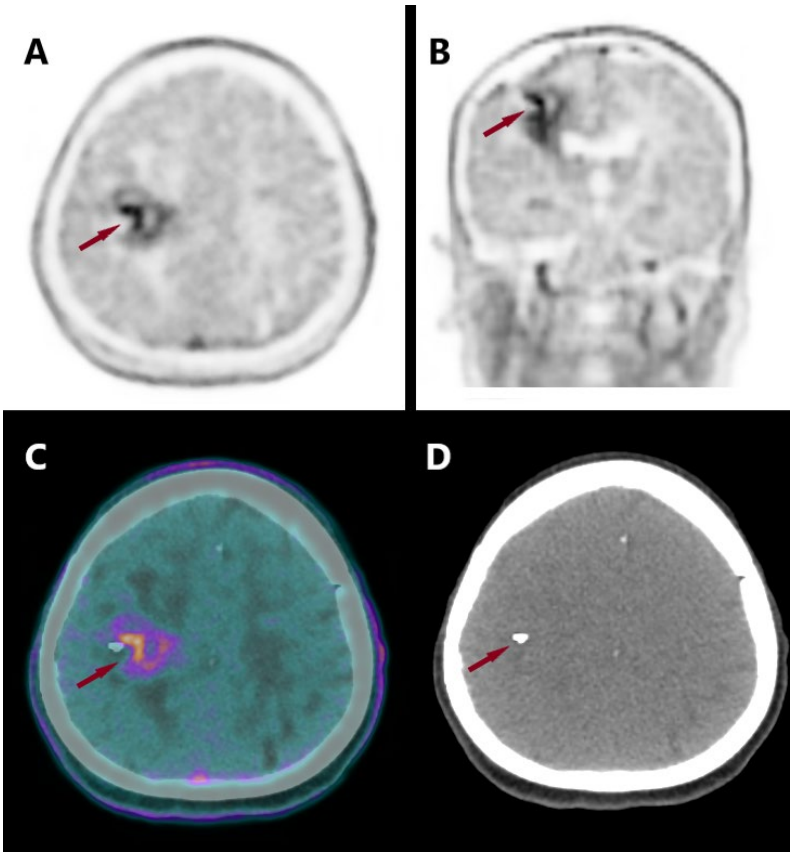

Figure 6: A 63-year-old female patient with relapsed glioblastoma WHO grade 4 IDH-wild type after surgical treatment for eleven months, radiotherapy for eight months, and adjuvant chemotherapy with temozolomide for four months. ^{18}F-FET PET/CT revealed a poly lobular lesion in the area of the precentral gyrus of the frontal right lobe, extending along the corona radiata to the corpus ventriculi lateralis, characterized by inhomogeneous accumulation of the tracer: moderately increased tracer accumulation along the periphery of the lesion and with the formation of "partitions" between metabolically inactive areas, which correspond to the zones of radiation necrosis. A lack of tracer uptake (red pointer) in its lateral part corresponds to postoperative changes and a maximum tracer accumulation in its dorsal part. CT (D) shows a metal clip in the area corresponding to the defect of tracer accumulation.

Several recent studies have analyzed the diagnostic utility of PET/CT with ^{18}F-FET in gliomas. According to these data, some new criteria for evaluation of the response of diffuse

gliomas using amino acid PET data were included in practice in January 2024, referred to as RANO PET 1.0 (76). These criteria are comparable to other published clinical MRI criteria and offer standardized protocols for imaging and post-processing of PET scans.

TBR displays the difference between tumors' metabolic activity and the physiological background, helping to distinguish between tumor recurrence and therapy-associated changes such as pseudoprogression.

Following the PET RANO criteria 1.0, several settings have been established for determining progression, disease stabilization, partial response, or complete response to treatment. The TBR value is necessary to determine the accuracy of the results. A positive ^{18}F-FET scan with the presence of viable tumor tissues, which allows for the registration of a metabolic active lesion and measurement of its volume, is considered at TBR >1.6. This value is present not only in the RANO criteria but also in the practice guidelines (77). However, in the study by Bashir et al. statistical analysis showed that thresholds of 2.0 for TBRmax, 1.8 for TBRmean, and 0.55 cm^3 for biological tumor volume (BTV) correlate with metabolic activity and potentially with tumor infiltration, while lower values are more indicative of non-tumorous processes; TBRmax showed precise performance (78).

Pseudoprogression is a well-known phenomenon which occurs particularly after combined radiochemotherapy. It represents a significant diagnostic challenge because it is difficult to distinguish from tumor recurrence using routine imaging, particularly MRI. The mechanism of this phenomenon is based on radiation-induced damage of the blood-brain barrier, endothelial cells, and oligodendroglia (79). Pseudoprogression is considered to be an excess response of irradiated tissue to therapy that is clinically manifested by edema, inflammation, and hypoxic stress. Morphologically, these changes may simulate tumor progression despite the absence of active tumor infiltration.

The clinical dilemma is that misinterpretation as recurrence may lead to unnecessary and potentially burdensome treatments such as reoperation or systemic therapy. Conversely, misdiagnosis of true progression as pseudoprogression may delay initiation of appropriate treatment. PET/CT with ^{18}F-FET has emerged as a promising diagnostic tool to visualize metabolic changes in gliomas. The accumulation of this tracer is based only on intracellular amino acid uptake and metabolism.

Still, the importance of the semi-quantitative parameter TBR remains insufficiently explored in differentiating relapse from pseudoprogression. The findings of this study may help to

improve protocols of non-invasive diagnostics and benefit the therapeutic outcomes in neuro-radiology.

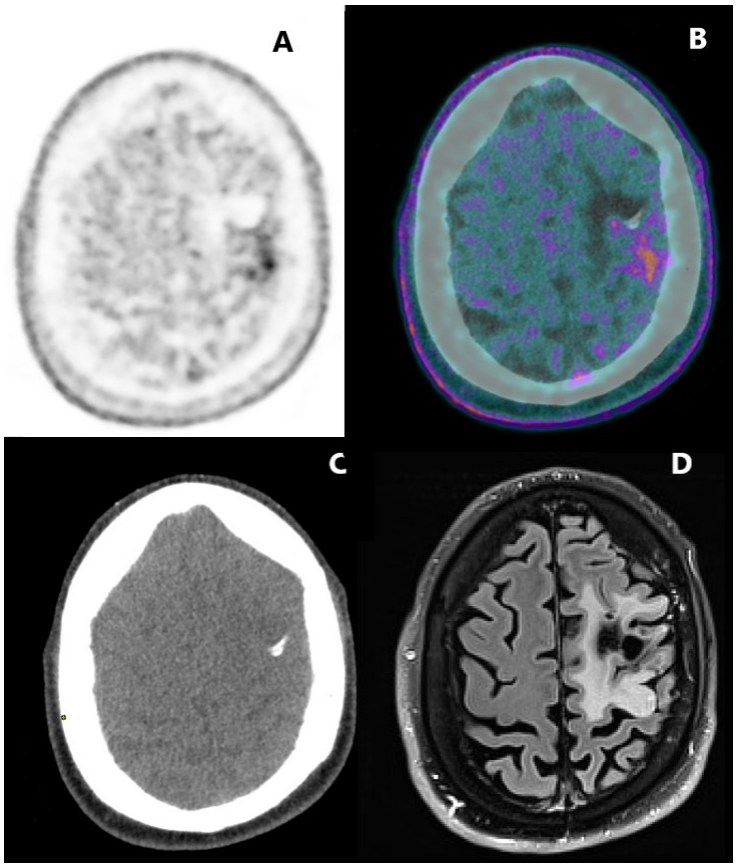

Figure 7: Comparison of the visualizing performance of diagnostic methods. Relapse of oligoastrocytoma WHO grade 4 in a 56-year-old male patient after two surgical treatments for 13 and 5 years and radiochemotherapy for 11 months. On PET/CT (A,B), the metabolic active lesion between the postcentral gyrus and the supramarginal gyrus of the left parietal lobe is characterized by an inhomogeneous accumulation of tracer with accentuation in its lateral-dorsal part. Ventral and medial located zones with practically minimal accumulation of tracer correspond to the area of surgical intervention. On CT (C), a metal clip is detected. On MRI (D), an extensive area of hyperintense signal on T2-FLAIR-sequence in the left parietal lobe was interpreted as postradiation edema or TRC.

5. Patients and Methods

5.1 Study design

The objective of our single-center retrospective study was to evaluate the statistical significance of semiquantitative PET parameters, especially tumor-to-brain ratio max and mean (TBRmax and TBRmean), in the re-diagnosis of glioma tumors at two-time points of dynamic acquisitions. Additionally, the study investigated the correlation of these parameters with histological characteristics of the tumor, such as WHO grade, and further possible implications for therapeutic decisions. TBR analysis was performed on tumor sections during two phases of ^{18}F-FET PET/CT acquisitions: early (10 min p.i.) and late (20-40 min p.i.).An inter-observer analysis was also performed between two physicians who independently reviewed the scans at early and late time phases for each WHO Grade of gliomas to determine which malignancy grade may be more challenging to process the scans and lead to potentially false identification of areas of interest. This would further affect the relevant calculation of semi-quantitative parameters. For the purpose of statistical processing, three values were derived: suspicious, which is characterized by a noticeable local or diffuse accumulation of tracer as determined by physicians; negative, which is defined as the absence of a pathologic accumulation of radiopharmaceutical; and equivocal, which is characterized by an implicit local or diffuse pattern of tracer that, which at purely visual evaluation does not allow to judge about the nature of these metabolic changes.

5.2 Participants

At our institution at the Medical University of Graz, Department of Radiology, Division of Nuclear Medicine, from July 1st, 2017, to October 31st, 2023, 218 ^{18}F-FET PET/CT primary and follow-up scans were performed in 198 patients. The inclusion criteria were:

- Histopathological confirmed glioma,
- Previous medical history of operation, radiotherapy and/or immunochemotherapy,
- Suspicion of recurrence/relapse of the primary disease or to clinical symptoms and/or MRI findings.

From the whole pool of patients, only 17/198 patients with 37 scans fit those criteria remained. One hundred eighty-one patients underwent only one ^{18}F-FET PET/CT scan. From the final pool with 37 scans, one patient with two scans was excluded with a

histological confirmed non-gestational Choriocarcinoma, leading to a final patient pool of 35 scans in 16 patients. See figure no. 8 chart-flow.

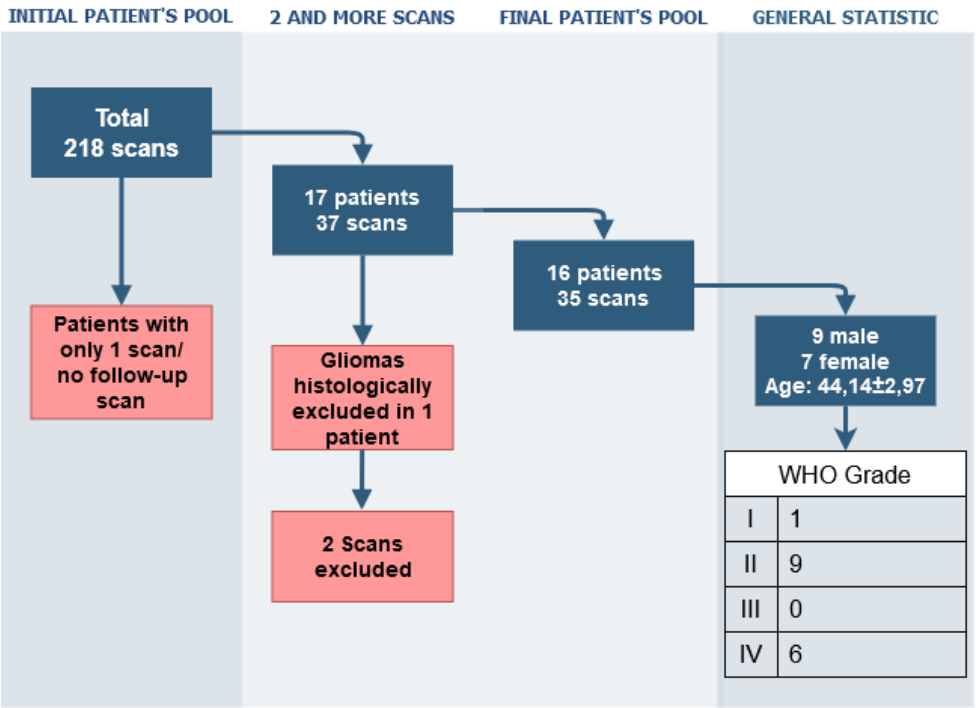

Figure 8: Patient selection chart for final sampling.

This study was conducted according to the principles of the Declaration of Helsinki and its subsequent amendments. The Ethics Committee at the Medical University of Graz (EK-number: 36-205 ex 23/24) granted approval. Since it was a retrospective study, written informed consent was waived.

It is worth mentioning that this retrospective study is conducted on the data pool of patients who underwent diagnostic procedures in the period before the revision of the WHO classification of tumors of the central nervous system occurred, in which the principle of tumor grading was slightly changed, making it closer to the grading system for non-CNS tumors. The introduction of grading within types allows for a more accurate prediction of the further course of the underlying disease and the prognosis of the outcome after complex treatment. The second innovation for the purpose of unification is related to the use of Arabic numerals for tumor grading (35). However, this study uses the old WHO 2016 classification, which was valid at the time of the study of the patients whose data are used in this study.

5.3 Equipment

All PET/CT examinations were performed on three dedicated PET/CT systems in 3D mode (Discovery MI, GE Healthcare, Milwaukee, WI, U.S.A.; Discovery ST, GE Healthcare, Milwaukee, WI, U.S.A.; and Biograph mCT, Siemens, Erlangen, Germany). Patients were unsystematically referred to each scanner.

5.4 ^{18}F-FET imaging and data acquisition

The amino acid ^{18}F-FET was synthesized and acquired from a certified third-party distributor. It was applied according to the established joint EANM/EANO/RANO practice guidelines (76,77).

PET/CT with ^{18}F-FET requires no unique and complex preparation. After a brief patient education and discussion of the potential risks of the procedure, which are very low, the patient is placed on the table in a supine position with the head fixed to minimize artifacts from potential head movement. All patients underwent dynamic PET scans after eating or complete fasting for at least 4 hours. All metallic items should be removed from the scanned region before the acquisition. The scans were performed with a single bed, with an axial field of view (AFOV) of 20 cm, i.e., the AFOV was placed on the patient's head. Before the dynamic emission acquisition was made, scout radiography and CT of the head were performed for AC. Dynamic acquisitions of the brain started simultaneously with intravenous radiopharmaceutical administration and were performed for 40 minutes. The target dose was 2 MBq/kg/body weight within a range of 114 – 240 MBq (202±26.57 MBq) according to established EANM dose recommendations (80).

This study aimed to evaluate two stages of dynamic acquisition using summarized static images from the early and late phases.

Because of the reconstruction parameters and post-processing steps, the different scanner types did not affect the quantitative ^{18}F-FET PET parameters (81).

At post-processing, the tracer's uptake in the tumor's region was determined by SUVmax using an automatic contouring process of VOI in 3 dimensions. The segmented volume and its threshold were afterward by an operator manually adjusted if there were within VOI any apparent non-tumor structures (e.g., sinus uptake).

TBRmax and TBRmean were calculated by dividing SUVmax and SUVmean of tumor's region to SUVmean of crescent-shaped ROI placed in the unaffected contralateral frontal lobe over gray and white matter (82). This algorithm of evaluation of TBR of affected regions in gliomas was conducted and recommended by the RANO group in PET RANO 1.0. It should be used for conducting future prospective clinical trials and in initial and follow-up scans.

For combined visual and semi-quantitative assessment, a TBRmax cut-off value of 1.6 was chosen to differentiate between TRC and TR. This number is recommended by current guidelines (76,77).

CT images and fused PET/CT images, which are obtained anyway, play no significant role in evaluating amino acid metabolism.

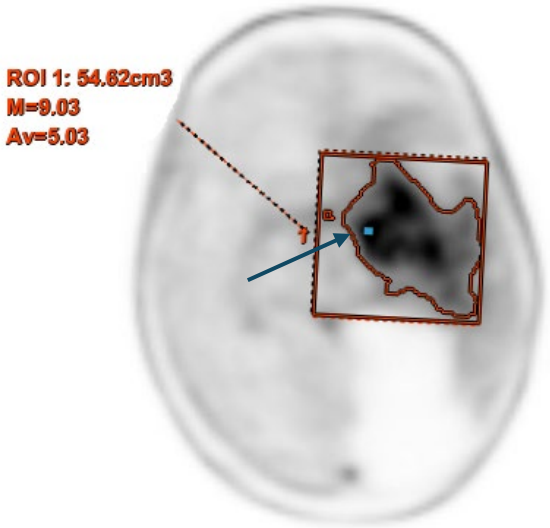

Figure 9: Measurement of SUVmax and SUVmean in ROI using automatic contouring. A blue point and arrow determine the maximum uptake point. The tumor's border (red contouring) is defined automatically. The ROI and their threshold should be estimated every time by an operator.

5.5 Disclaimer

All procedures performed in this study were in accordance with the principles of the Declaration of Helsinki and its further amendments and with the ethical standards of the institutional research committee (Ethikkommission der Medizinischen Universität Graz – Ethics Committee at Medical University of Graz (application number: 36-205 ex 23/24, approval date: March 3rd, 2024)). Being a retrospective study, the need for written informed consent was waived.

6. Results

Seventeen patients underwent two or more PET scans at different time intervals after treatment. The study included patients with histopathologically confirmed glioma with suspected recurrence after surgical treatment and/or radiation therapy. See figure no. 8 chart-flow.

In our patient collective, 9/16 patients (56%) were male, and 7/16 (44%) were female, with a median age of 45 years. More than half of the final patient pool had a glioma WHO grade 2, while no WHO grade 3 was present. All 16 patients had previously received chemo- or/and immunotherapy with mainly temozolomide, lomustin, or bevacizumab; 10/16 patients (56%) had a history of operation, while 15/16 patients (94%) had radiation therapy performed previously. See Table 4 for patient characteristics.

The statistical analysis was performed using Microsoft Excel (Microsoft) and SPSS v.28 (IBM). A P-value below 0.05 was regarded as statistically significant.

		Mean	**Standard Deviation**
Age		44	17.59
Sex			
Men	n	9	
Women	n	7	
Height	cm	168	13.18
Weight	kg	65	21.04
Activity of ^{18}F-FET	MBq	191.32	26.31
WHO grade	1	n = 1	6%
	2	n = 9	56%
	3	n = 0	0%
	4	n = 6	38%

Table 4: **Descriptive statistics of the final patient's pool characteristics.**

In the early phase, SUVmax had a median value of 3.78, rising to a median of 5.20 in the late acquisitions. Similarly, SUVmean rose from 1.90 in the early acquisitions to 2.69 in the late acquisitions. The median MTV rose from 7.63 to 12.2, although a large range was observed, especially in the late acquisition, ranging from 3.12 to 147.0 cm³. As it turned out in the analysis, numerical changes of semiquantitative parameters TBRmax and TBRmean

have a multidirectional trend. TBRmax increases from 2.43 in the early phase to 2.8 in the late phase, rise to 15%. Hence, TBRmean drops from 2.28 to 2.20, with a drop of 13%. For more detailed information, see Table 5.

Early phase (0-10 min p.i.)	**SUVmax**	**SUVmean**	**MTV (cm³)**	**TBRmax**	**TBRmean**
Mean	4.45	2.25	7.63	2.79	2.39
Geometric mean	3.90	2.00	8.36	2.53	2.20
Median	3.78	1.90	7.63	2.43	2.28
Standard deviation	2.55	1.17	10.17	1.31	0.98
Minimum	1.60	0.80	1.50	1.10	1.11
Maximum	11.00	5.64	42.93	6.63	5.42
Late phase (20-40 min p.i.)	**SUVmax**	**SUVmean**	**MTV (cm³)**	**TBRmax**	**TBRmean**
Mean	5.53	3.04	20.91	2.87	2.18
Geometric mean	5.02	2.78	13.19	2.67	2.06
Median	5.20	2.69	12.2	2.80	2.20
Standard deviation	2.79	1.37	28.29	1.07	0.72
Minimum	2.23	1.35	3.12	1.37	1.00
Maximum	12.92	7.31	147.00	4.95	3.77

Table 5: Descriptive statistics of different semi-quantitative PET parameters acquired for early and late acquisition.

Twenty-five scans out of 35 (71%) were assessed as PET-positive disease in terms of progression, stable disease, and recurrence after therapy.

Four out of 16 patients (25%) with PET-positive assessed scans underwent second surgical treatment, and 8 out of 16 (50%) underwent re-RT.

In our cohort, 4 out of 35 (11%) cases were diagnosed by MRI with TRC after treatment, but ^{18}F-FET PET/CT demonstrated these results as progression. In the early phase, the median SUVmax value reached 4.56, and the SUVmean was 2.50, while in the late phase, the SUVmax was 6.50 and the SUVmean 3.14. For the early phase, the semi-quantitative parameters TBRmax and TBRmean reached the same value of 2.91, and in the late phases, TBRmax was 3.54, and TBRmean was 2.51.

The opposite situation was observed in 7 out of 35 cases (20%) when TR was determined according to the MRI data when unexpressed amino acid metabolism was noted on PET/CT images with FET analogs. TBRmax and TBRmean at the early phase reached 1.78 and 1.43,

respectively. In the late stage, TBRmax and TBR mean parameters possess 1.75 and 1.52 values, respectively.

Early phase (0-10 min p.i.)	**SUVmax**	**SUVmean**	**MTV (cm³)**	**TBRmax**	**TBRmean**
Mean	5.15	2.98	7.10	3.33	2.93
Geometric mean	4.78	2.57	7.04	3.17	2.83
Median	4.56	2.50	7.10	2.91	2.91
Standard deviation	3.48	1.90	0.99	1.28	0.90
Minimum	2.59	1.29	1.59	2.36	2.02
Maximum	10.35	5.63	8.19	5.15	3.91
Late phase (20-40 min p.i.)	**SUVmax**	**SUVmean**	**MTV (cm³)**	**TBRmax**	**TBRmean**
Mean	7.45	3.94	16.04	3.51	2.58
Geometric mean	6.75	3.53	13.20	3.48	2.56
Median	6.50	3.14	11.78	2.80	2.20
Standard deviation	3.93	2.30	12.28	0.53	0.42
Minimum	3.89	2.18	6.7	2.95	2.20
Maximum	12.92	7.31	33.90	4.01	3.10

Table 6: Descriptive statistics of different semi-quantitative PET parameters by patients with assessed stabilization or TRC on MRI scans, hence on PET/CT as a TR.

Early phase (0-10 min p.i.)	**SUVmax**	**SUVmean**	**MTV (cm³)**	**TBRmax**	**TBRmean**
Mean	2.82	1.58	8.46	1.66	1.68
Geometric mean	2.74	1.52	6.37	1.61	1.62
Median	2.50	1.3	8.42	1.78	1.43
Standard deviation	0.83	0.49	5.85	0.44	0.53
Minimum	2.29	1.25	1.5	1.10	1.23
Maximum	4.47	2.48	16.32	2.19	2.61
Late phase (20-40 min p.i.)	**SUVmax**	**SUVmean**	**MTV (cm³)**	**TBRmax**	**TBRmean**
Mean	3.80	2.12	11.67	1.93	1.58
Geometric mean	3.70	2.03	10.23	1.90	1.56
Median	3.53	2.0	15.06	1.75	1.52
Standard deviation	0.99	0.70	5.89	0.37	0.27
Minimum	2.87	1.35	5.01	1.56	1.36
Maximum	5.2	2.99	17.16	2.46	2.04

Table 7: Descriptive statistics of semi-quantitative PET parameters by patients assessed on MRI scans as TR, whereas on PET/CT as TRC.

In three cases, there was a discordance between the MRI findings and the PET/CT results. At the endpoint of this study, 7/16 patients (44%) had died due to glioma-related causes, while the remaining 9/16 patients (56%) were under ongoing surveillance.

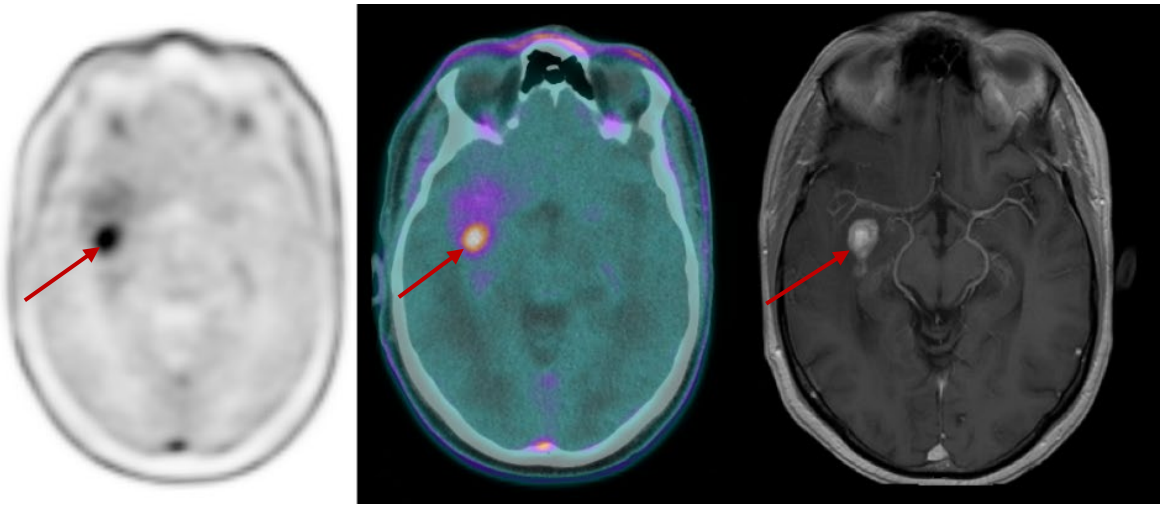

Figure 10: Relapse astrocytoma WHO 2 grade in a 48-year-old male patient after two courses of radiotherapy for 19 months and 18 cycles of chemotherapy. Left/middle panel: oval inhomogeneous accumulation of ^{18}F-FET in the posterior right insula with the maximum uptake focus in the dorsal part (red arrow) corresponding to disease relapse. Right panel: hyperintense signal on T1 contrast-weighted images assessed as radiation necrosis.

To assess the specifics of the relationship between WHO tumor grade and the TBRmax and TBRmean values at different phases, correlation analysis (quantitative, non-parametric test with Spearman's correlation) was conducted. The correlation analysis results are shown in Tab. 8. Thus, based on the data presented in the table, a reliable correlation between semi-quantitative parameters and WHO grades was found only for TBRmean in the early phase. The confidence level was p = 0.0180, the correlation coefficient was moderate, and R = 0.4092. For the other parameters, there was no reliable relationship.

	R Spearman	P-value
TBRmax early	0.2463	0.1671
TBRmean early	0.4092	0.0180
TBRmax late	0.1086	0.5540
TBRmean late	0.2799	0.1207

Table 8: Correlation analysis between WHO grading and TBR.

Similarly, a correlation analysis using Spearman's rank correlation coefficient was performed to determine the correlation between TBRmax, TBRmean, and re-treatment.

Accordingly, the data illustrated in Tab. 9 indicated that no relationships between these parameters were considered in this investigation.

	R Spearmen	P-value
TBRmax early	0.2085	0.2442
TBRmean early	0.0606	0.7377
TBRmax late	0.0854	0.6419
TBRmean late	-0.0157	0.9319

Table 9: Correlation analysis between re-operation/re-radiation therapy and TBR

Next, all patients were divided into subgroups according to the WHO parameter value (group 1 - WHO = 1; group 2 - WHO = 2, etc.) and the groups were compared with each other by Tumor-to-Brain Ratio (TBRmax and TBRmax early and late phases). The comparison was performed using the nonparametric Kruskal-Wallis-Test, which compares independent samples when there are more than two groups. As a result of the comparison, no significant differences were observed (for TBRmax early, the level of confidence was p = 0.3076; for TBRmean early, p = 0.1511 and for TBRmax late and TBRmean late, the level of confidence was p = 0.3114).

Interobserver analysis

A frequency analysis was performed to compare data on visual assessments by two nuclear medicine physicians in the early and late phases. We calculated the absolute number of grades ("Abs." columns), their proportion of the total number of grades ("%" columns) and compared the frequency of occurrence of each grading option between the two physicians (Tab. 10). The two nuclear medicine physicians' scores for the frequency of occurrence of each variant were identical (level of difference - "p" column equal to 1.0, except for the variant "suspect" in the "late" scores, where no reliability was also observed, p=0.7851).

	Early 1		Early 2		P-value	Late 1		Late 2		P-value
	Abs.	%	Abs.	%		Abs.	%	Abs.	%	
equivocal	8	22.9%	9	25.7%	1.0000	4	11.4%	3	8.6%	1.0000
negative	7	20.0%	7	20.0%	1.0000	6	17.1%	5	14.3%	1.0000
suspect	20	57.1%	19	54.3%	1.0000	25	71.4%	27	77.1%	0.7851

Table 10: Frequency analysis visual assessment of interobserver analysis (2x2 tables, Fisher's test, two-sided). 1- visual analysis of the first physician. 2- visual analysis of the second physician.

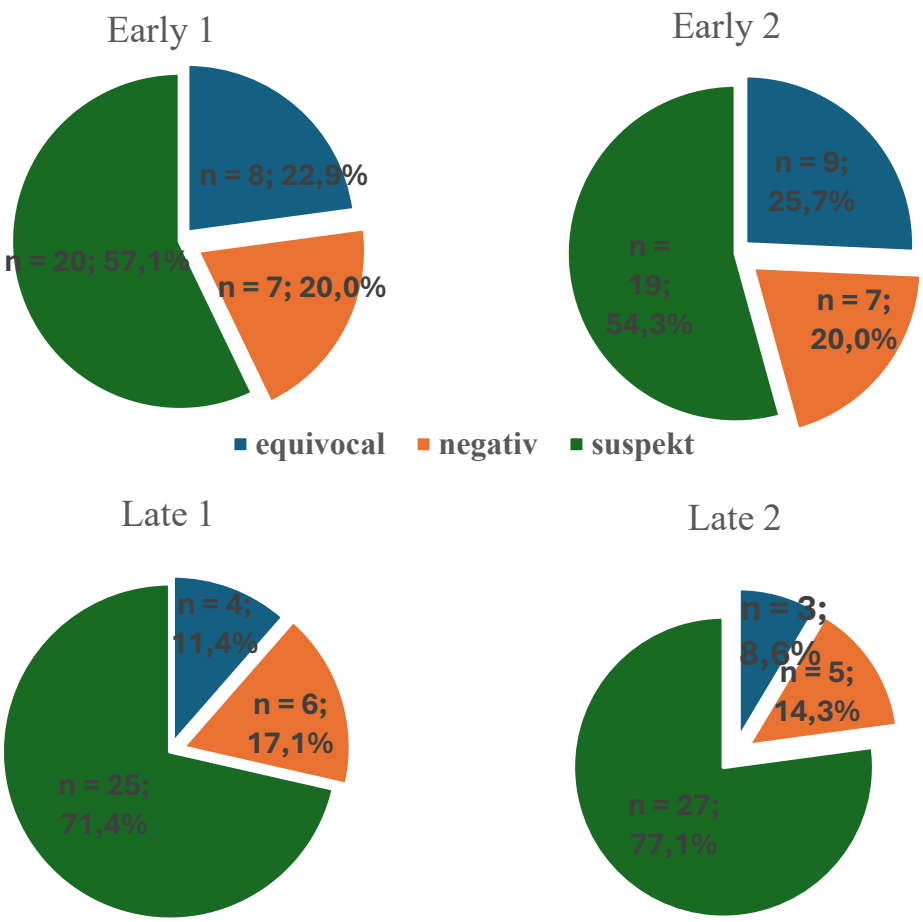

Figure 11: Visual display of frequency analysis of interobserver evaluation (see Table 10).

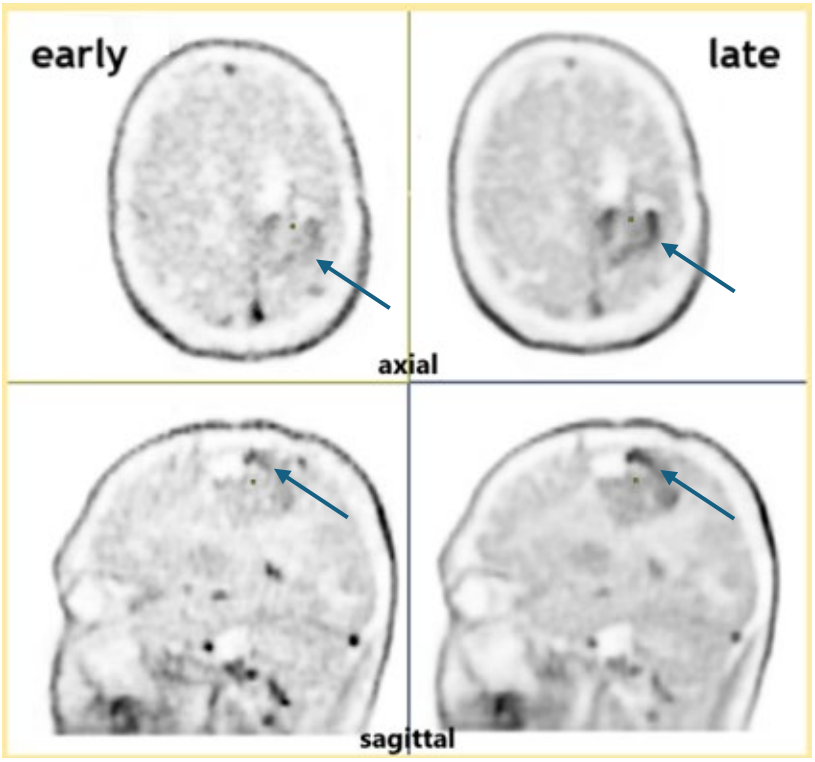

Figure 12: Visual comparison of tracer accumulation and distribution in ^{18}F-FET PET/CT in two-time intervals on scans of a 56-year-old male patient with astrocytoma WHO grade 4 on axial and sagittal planes. Visually, a more intense tracer accumulation in areas of interest (blue arrows) is determined over time. The intensity of the blood pool at the late stage decreases naturally, which is related to the molecular mechanism of amino acid uptake by LAT1.

Finally, the visual assessments were compared using the non-parametric statistics method with the Wilcoxon test, which showed no significant difference. The significance level of differences between “Late 1” and “Late 2” was $p = 0.5049$. The level of significance between “Early 1” and “Early 2 " suggests a tendency for a significant difference ($p = 0.0641$).

7. Discussion

Gliomas are a heterogeneous group of tumors that still raise significant challenges in diagnosis and treatment and need a multidisciplinary approach by neurologists, neurosurgeons, radiotherapists, pathologists, and imaging physicians. MRI is applied primarily for the initial diagnosis and follow-up studies since it is now available and has more than 15 years of standardized protocol for study interpretation. However, PET/CT with amino acid analogs as a relatively novel molecular imaging modality can provide valuable diagnostic information on follow-up imaging in patients with glioma. Improved diagnostic accuracy offers a better insight into the impact of treatment, which improves the management strategies.

The aim of our retrospective study was to analyze the semi-quantitative parameters TBRmax and TBRmean in ^{18}F-FET PET/CT evaluated in two scanning time phases in patients with histologically confirmed gliomas with suspected glioma recurrence. Mean TBRmax in the late phase rises around 15% when the mean numerical of TBRmean drops to 13%. These variations should not be recognized as statistically significant, as they may relate to the average increased physiological accumulation in normal brain tissues. In fact, there is a more substantial amount of detected activity in the late phase compared to the early phase. The main aim was to statistically ascertain whether there is a difference in these parameters at different time points, in which case an adaptation of the acquisition algorithms with a possible reduction in total scan time would be feasible.

The statistically moderate correlation between the semi-quantitative TBRmean at the early phase and tumor grade found in our study should be regarded. However, the absence of grade 3 glioma in our sample limits the validity of this correlation, so further large-scale studies are needed to confirm this relationship. The final statistical analysis did not reveal any statistically significant association between the values of studied parameters in both time phases. The small sample of patients for the design of this study limits the possibility of generalizing the obtained results.

The diagnostic value of visualizing amino acid metabolism with ^{18}F-FET is very high, with sensitivity and specificity reaching 91% and 100%, respectively (74). Therefore, nuclear medicine diagnostics with ^{18}F-FET PET/CT can be helpful in cases where histological examination is not possible or uncertain. Information on molecular characteristics, e.g.,

predicting IDH status and glioma grading, may have implications for treatment strategies, as explored in the scientific literature (48,81,83–85).

To determine the histologic characterization of gliomas, for example, WHO grade, according to a meta-analysis by Katsanos et al. (73), PET diagnostics with MET and FET show a high sensitivity of 94% and 88%, respectively. The specificity of the method with these tracers is about 56%, but their combination with another nuclear imaging modality, such as ^{18}F-FDG PET/CT, reaches 89%.

The complex pathophysiology of the illness makes the diagnosis and follow-up of gliomas truly challenging in clinical practice. Following the publication of RANO PET guidelines 1.0 (76) nuclear imaging has been increasingly included in the diagnostics list. However, MRI is still traditionally the mainstay tool for diagnosis. However, accurate differentiation of TR from TRC remains critical for further treatment strategy and also challenging in follow-up diagnosis of gliomas. Therefore, a precise understanding of progression, pseudoprogression, pseudoreaction, and radiation necrosis is required. The dilemma is that misinterpreting as a recurrence can lead to unnecessary and potentially burdensome therapies such as repeat surgery or systemic therapy. Conversely, misjudgment of true progression as pseudoprogression could lead to delayed adequate treatment. On MRI TRCs, including pseudoprogression and radiation necrosis, radiologically often present with features suggesting tumor recurrence, such as signal changes, especially on T1 and T2 sequences and contrast enhancement, because of the damaged brain-blood barrier. Primarily, TRCs represent radiation-induced brain edema, which is most prominent during the first three months after radiotherapy. It is necessary to hold this observation period to better determine the effectiveness of treatment of a patient with high-grade glioma (86).

^{18}F-FET PET/CT has emerged as a promising diagnostic tool that can visualize metabolic changes in gliomas. Imaging with ethyltyrosine relies on increased amino acid uptake by tumor cells via L-amino acid transporters. It provides excellent contrast between tumor and background and low background uptake in normal brain tissue, distinguishing metabolically active tumor tissue from post-treatment necrosis or inflammatory changes. Quantitative parameters in ^{18}F-FET PET/CT, particularly TBR, have been shown to be crucial tools for distinguishing actual responses and treatment-related changes. Sensitivity and specificity reach 91-100% and 84-86%, respectively (87,88).

Compared to MRI, ^{18}F-FET PET shows a significantly higher diagnostic performance with accuracy of 93% and 85% by MRI. A study by Verger et al. (89) showed a significant diagnostic power of ^{18}F-FET PET using TBRmax to differentiate between TRC and progressive or recurrent glioma. At the same time, none of the perfusion-weighted MRI parameters reached significance.

The retrospective study also aimed to evaluate the possible impact of these semi-quantitative parameters on therapeutic decisions in patients with histologically confirmed gliomas. The study illustrated that the semi-quantitative parameter TBR differentiates between TRC and TR, which is helpful in guiding treatment decision.

MRI results were negative in three cases out of the total number of patients. Still, PET/CT with ^{18}F-FET showed a significant level of tyrosine analog uptake in previously affected brain regions. This led to the conclusion of disease progression, which was the basis for changing the therapeutic regimen.

In twelve cases, scan results of PET/CT with ^{18}F-FET directly influenced therapeutic decisions in our patient's cohort, including re-irradiation and, in some cases, reoperation. In the rest, positive PET/CT results played a supporting role and were concordant with MRI findings.

Four cases were assessed on MRI as TRC, which preceded nuclear imaging. When PET/CT scans were performed, and a semiquantitative assessment of standard parameters was conducted, the findings were interpreted as TR with a median TBR in the two-time phases exceeding the recommended threshold of 1.6 set by guidelines (76,77)

In the seven cases where MRI scans were interpreted as TR, the TBRmax values in the two-time phases also exceeded the threshold of 1.6 by an average of 10.3%, while TBRmean was below this threshold. Established scan results were interpreted as TRC. The data varied not significantly from the established ones, but the disagreement indicates the necessity of complex analysis of semi-quantitative parameters in follow-up studies with known baseline data. For example, if MRI data shows preserved or increased areas of altered signal, but with TBRmax decreasing by more than 30% and TBRmean less than 10% from the baseline, then the detected changes correspond to partial response, and the preserved or appeared areas of altered signal on MRI can be interpreted as TRC.

Considering that the study's main aim was to evaluate semi-quantitative parameters at different time points, it is also worth discussing the significance of time parameters of dynamic PET/CT with tyrosine in the diagnosis of glioma, which is still insufficiently studied in scientific literature. Several studies (90–92) have investigated the diagnostic utility of TBR and dynamic parameter time to peak (TTP) indices in predicting tumor molecular profiles, including IDH-wildtype or mutant status and the presence of TERTp mutations, where invasive diagnostic was impossible to perform. For instance, Vettermann, F. et al. assessed (90) semiquantitative parameter TBRmax scores in predicting glioma molecular phenotype, particularly TERTp mutation at 5-15 min and 20–40-min intervals, whereas our study, without regard to prediction of the genetic type of the tumor, concentrated on 0-10 min and 20–40-min intervals. While TBR scores alone lack prognostic value, dynamic scores such as TTP were found to possess more excellent prognostic value in (87).

Since few studies using two-time points have been performed, it can be reasonably argued that this area of research requires intensive methodological development to explore further the relationship of TTP parameters for determining the molecular nature of glioma tumors with therapeutic outcomes.

While ^{18}F-FET shows promise as a complementary modality to MRI in the management of primary and metastatic brain malignancies, further validation with standardized image interpretation methods in well-designed prospective studies is warranted. In addition, the use of PET/CT with this tracer for primary diagnosis is accompanied by high economic costs; therefore, its use as the preferred standard diagnostic tool remains questionable, as MRI is the more available diagnostic method.

Gliomas are a heterogeneous group of tumors characterized by different growth rates and infiltrative behavior. Therefore, nuclear imaging using amino acid tracers requires a consistently validated algorithm for image interpretation. With systematic data analysis, this method will be a valid diagnostic tool if the data are analyzed consistently. Therefore, we evaluated interobserver agreement when interpreting scans of glioma with suspected recurrence. No statistical significance was found regarding the WHO grades of tumors, but we found a substantial interobserver agreement for ^{18}F-FET PET/CT evaluation in glioma recurrence. The high interobserver agreement may be reached by strict adherence to the defined image interpretation criteria.

8. Conclusion

^{18}F-FET PET/CT is a newly established reliable molecular imaging method in diagnosing gliomas and offers high diagnostic value. This retrospective study for evaluating the value of semi-quantitative ^{18}F-FET PET/CT parameters showed no statistical significance at two-time points. Only a moderate correlation between TBRmean values in the early phase and WHO grade was present. The absence of WHO grade III tumors in the patient cohort questions the credibility of this observation.

Using the generally accepted semiquantitative parameter TBR with a cut-off of 1.6 is crucial for differentiating TRC (pseudoprogression, pseudoreaction, and radionecrosis) from TR in cases with equivocal MRI findings. This improves the management of gliomas.

Further prospective studies should consider and evaluate the role of semiquantitative PET/CT parameters at different time points in diagnosing glioma. These studies should also include dynamic parameters like TTP, which can help with more accurate noninvasive diagnostics and determination of the prognostic probability. Standardized image interpretation should also be established.

9. References

1. Chen R, Smith-Cohn M, Cohen AL, Colman H. Glioma Subclassifications and Their Clinical Significance. Neurotherapeutics. April 2017;14(2):284–97.

2. Wang LM, Englander ZK, Miller ML, Bruce JN. Malignant Glioma. In: Rezaei N, Hanaei S, Herausgeber. Human Brain and Spinal Cord Tumors: From Bench to Bedside Volume 2 [Internet]. Cham: Springer International Publishing; 2023 [zitiert 26. März 2025]. S. 1–30. (Advances in Experimental Medicine and Biology; Bd. 1405). Verfügbar unter: https://link.springer.com/10.1007/978-3-031-23705-8_1

3. Hackl M, Ihle P. Krebserkrankungen in Österreich 2022 [Internet]. 2022 [zitiert 29. März 2025]. Verfügbar unter: https://www.statistik.at/fileadmin/publications/Krebserkrankungen_2022.pdf

4. Ostrom QT et al: Epidemiology of Gliomas. In: Cancer Treatment and Research [Internet]. Cham: Springer International Publishing; 2015 [zitiert 29. März 2025]. S. 1–14. Verfügbar unter: https://link.springer.com/10.1007/978-3-319-12048-5_1

5. Ostrom QT, Cioffi G, Waite K, Kruchko C, Barnholtz-Sloan JS. CBTRUS Statistical Report: Primary Brain and Other Central Nervous System Tumors Diagnosed in the United States in 2014–2018. Neuro-Oncol. 5. Oktober 2021;23(Supplement_3):iii1–105.

6. Vigneswaran K, Neill S, Hadjipanayis CG. Beyond the World Health Organization grading of infiltrating gliomas: advances in the molecular genetics of glioma classification. Ann Transl Med. Mai 2015;3(7):95.

7. Cote DJ, Ostrom QT, Gittleman H, Duncan KR, CreveCoeur TS, Kruchko C, u. a. Glioma incidence and survival variations by county-level socioeconomic measures. Cancer. Oktober 2019;125(19):3390–400.

8. McNeill KA. Epidemiology of Brain Tumors. Neurol Clin. November 2016;34(4):981–98.

9. Davis ME. Epidemiology and Overview of Gliomas. Semin Oncol Nurs. Dezember 2018;34(5):420–9.

10. Ellor SV, Pagano-Young TA, Avgeropoulos NG. Glioblastoma: Background, Standard Treatment Paradigms, and Supportive Care Considerations. J Law Med Ethics. 2014;42(2):171–82.

11. Johnson DR, Fogh SE, Giannini C, Kaufmann TJ, Raghunathan A, Theodosopoulos PV, u. a. Case-Based Review: newly diagnosed glioblastoma. Neuro-Oncol Pract. 1. September 2015;2(3):106–21.

12. Alifieris C, Trafalis DT. Glioblastoma multiforme: Pathogenesis and treatment. Pharmacol Ther. August 2015;152:63–82.

13. Hottinger AF, Khakoo Y. Update on the management of familial central nervous system tumor syndromes. Curr Neurol Neurosci Rep. Mai 2007;7(3):200–7.

14. Gu J, Liu Y, Kyritsis AP, Bondy ML. Molecular Epidemiology of Primary Brain Tumors. Neurotherapeutics. Juli 2009;6(3):427–35.

15. Forsyth PA, Posner JB. Headaches in patients with brain tumors: A study of 111 patients. Neurology. September 1993;43(9):1678–1678.

16. Mesfin FB, Karsonovich T, Al-Dhahir MA. Gliomas. In: StatPearls [Internet]. Treasure Island (FL): StatPearls Publishing; 2025 [zitiert 29. März 2025]. Verfügbar unter: http://www.ncbi.nlm.nih.gov/books/NBK441874/

17. Schaff LR, Mellinghoff IK. Glioblastoma and Other Primary Brain Malignancies in Adults: A Review. JAMA. 21. Februar 2023;329(7):574–87.

18. Chen H, Judkins J, Thomas C, Wu M, Khoury L, Benjamin CG, u. a. Mutant IDH1 and seizures in patients with glioma. Neurology. 9. Mai 2017;88(19):1805–13.

19. Gil-Gil MJ, Mesia C, Rey M, Bruna J. Bevacizumab for the treatment of glioblastoma. Clin Med Insights Oncol. 2013;7:123–35.

20. Walbert T, Harrison RA, Schiff D, Avila EK, Chen M, Kandula P, u. a. SNO and EANO practice guideline update: Anticonvulsant prophylaxis in patients with newly diagnosed brain tumors. Neuro-Oncol. 2. November 2021;23(11):1835–44.

21. Avila EK, Chamberlain M, Schiff D, Reijneveld JC, Armstrong TS, Ruda R, u. a. Seizure control as a new metric in assessing efficacy of tumor treatment in low-grade glioma trials. Neuro-Oncol. Januar 2017;19(1):12–21.

22. Davis ME. Glioblastoma: Overview of Disease and Treatment. Clin J Oncol Nurs. 1. Oktober 2016;20(5 Suppl):S2-8.

23. Lim-Fat MJ, Bi WL, Lo J, Lee EQ, Ahluwalia MS, Batchelor TT, u. a. Letter: When Less is More: Dexamethasone Dosing for Brain Tumors. Neurosurgery. 1. September 2019;85(3):E607–8.

24. Perry JR. Thromboembolic disease in patients with high-grade glioma. Neuro-Oncol. September 2012;14 Suppl 4(Suppl 4):iv73-80.

25. Iorio A, Agnelli G. Low-molecular-weight and unfractionated heparin for prevention of venous thromboembolism in neurosurgery: a meta-analysis. Arch Intern Med. 14. August 2000;160(15):2327–32.

26. Grossman R, Mukherjee D, Chang DC, Bennett R, Brem H, Olivi A, u. a. Preoperative charlson comorbidity score predicts postoperative outcomes among older intracranial meningioma patients. World Neurosurg. Februar 2011;75(2):279–85.

27. Luna LP, Sherbaf FG, Sair HI, Mukherjee D, Oliveira IB, Köhler CA. Can Preoperative Mapping with Functional MRI Reduce Morbidity in Brain Tumor Resection? A Systematic Review and Meta-Analysis of 68 Observational Studies. Radiology. August 2021;300(2):338–49.

28. Thakkar JP, Dolecek TA, Horbinski C, Ostrom QT, Lightner DD, Barnholtz-Sloan JS, u. a. Epidemiologic and molecular prognostic review of glioblastoma. Cancer Epidemiol Biomark Prev Publ Am Assoc Cancer Res Cosponsored Am Soc Prev Oncol. Oktober 2014;23(10):1985–96.

29. Walid MS. Prognostic factors for long-term survival after glioblastoma. Perm J. 2008;12(4):45–8.

30. Sherman JC, Colvin MK, Mancuso SM, Batchelor TT, Oh KS, Loeffler JS, u. a. Neurocognitive effects of proton radiation therapy in adults with low-grade glioma. J Neurooncol. Januar 2016;126(1):157–64.

31. Hanna C, Lawrie TA, Rogozińska E, Kernohan A, Jefferies S, Bulbeck H, u. a. Treatment of newly diagnosed glioblastoma in the elderly: a network meta-analysis. Cochrane Database Syst Rev. 23. März 2020;3(3):CD013261.

32. Vatnitsky S, Rosenblatt E. Transition from 2-D radiotherapy to 3-D conformal and intensity modulated radiotherapy. Vienna: International Atomic Energy Agency; 2008.

33. Barani IJ, Larson DA. Radiation therapy of glioblastoma. Cancer Treat Res. 2015;163:49–73.

34. Louis DN, Ohgaki H, Wiestler OD, Cavenee WK, Burger PC, Jouvet A, u. a. The 2007 WHO Classification of Tumours of the Central Nervous System. Acta Neuropathol (Berl). August 2007;114(2):97–109.

35. Louis DN, Perry A, Wesseling P, Brat DJ, Cree IA, Figarella-Branger D, u. a. The 2021 WHO Classification of Tumors of the Central Nervous System: a summary. Neuro-Oncol. 2. August 2021;23(8):1231–51.

36. Omuro A, DeAngelis LM. Glioblastoma and other malignant gliomas: a clinical review. JAMA. 6. November 2013;310(17):1842–50.

37. Ostrom QT, Gittleman H, Truitt G, Boscia A, Kruchko C, Barnholtz-Sloan JS. CBTRUS Statistical Report: Primary Brain and Other Central Nervous System Tumors Diagnosed in the United States in 2011-2015. Neuro-Oncol. 1. Oktober 2018;20(suppl_4):iv1–86.

38. Becker KP, Yu J. Status quo--standard-of-care medical and radiation therapy for glioblastoma. Cancer J Sudbury Mass. 2012;18(1):12–9.

39. Oronsky B, Reid TR, Oronsky A, Sandhu N, Knox SJ. A Review of Newly Diagnosed Glioblastoma. Front Oncol. 2020;10:574012.

40. Rudà R, Pellerino A, Magistrello M, Franchino F, Pinessi L, Soffietti R. Molecularly based management of gliomas in clinical practice. Neurol Sci Off J Ital Neurol Soc Ital Soc Clin Neurophysiol. September 2015;36(9):1551–7.

41. Fang Q. The Versatile Attributes of MGMT: Its Repair Mechanism, Crosstalk with Other DNA Repair Pathways, and Its Role in Cancer. Cancers. 11. Januar 2024;16(2):331.

42. Cankovic M, Nikiforova MN, Snuderl M, Adesina AM, Lindeman N, Wen PY, u. a. The Role of MGMT Testing in Clinical Practice. J Mol Diagn. September 2013;15(5):539–55.

43. Siegal T. Clinical Relevance of Prognostic and Predictive Molecular Markers in Gliomas. Adv Tech Stand Neurosurg. 2016;(43):91–108.

44. Yan H, Parsons DW, Jin G, McLendon R, Rasheed BA, Yuan W, u. a. *IDH1* and *IDH2* Mutations in Gliomas. N Engl J Med. 19. Februar 2009;360(8):765–73.

45. Jenkins RB, Blair H, Ballman KV, Giannini C, Arusell RM, Law M, u. a. A t(1;19)(q10;p10) Mediates the Combined Deletions of 1p and 19q and Predicts a Better

Prognosis of Patients with Oligodendroglioma. Cancer Res. 15. Oktober 2006;66(20):9852–61.

46. van den Bent MJ, Wefel JS, Schiff D, Taphoorn MJB, Jaeckle K, Junck L, u. a. Response assessment in neuro-oncology (a report of the RANO group): assessment of outcome in trials of diffuse low-grade gliomas. Lancet Oncol. Juni 2011;12(6):583–93.

47. Wu J, Su R, Qiu D, Cheng X, Li L, Huang C, u. a. Analysis of DWI in the classification of glioma pathology and its therapeutic application in clinical surgery: a case-control study. Transl Cancer Res. April 2022;11(4):805–12.

48. Thust SC, van den Bent MJ, Smits M. Pseudoprogression of brain tumors. J Magn Reson Imaging JMRI. 7. Mai 2018;48(3):571–89.

49. Wen PY, Van Den Bent M, Youssef G, Cloughesy TF, Ellingson BM, Weller M, u. a. RANO 2.0: Update to the Response Assessment in Neuro-Oncology Criteria for High- and Low-Grade Gliomas in Adults. J Clin Oncol. 20. November 2023;41(33):5187–99.

50. Qin D, Yang G, Jing H, Tan Y, Zhao B, Zhang H. Tumor Progression and Treatment-Related Changes: Radiological Diagnosis Challenges for the Evaluation of Post Treated Glioma. Cancers. 3. August 2022;14(15):3771.

51. Thenuwara G, Curtin J, Tian F. Advances in Diagnostic Tools and Therapeutic Approaches for Gliomas: A Comprehensive Review. Sensors. 15. Dezember 2023;23(24):9842.

52. Phelps ME. PET: the merging of biology and imaging into molecular imaging. J Nucl Med Off Publ Soc Nucl Med. April 2000;41(4):661–81.

53. Cherry SR, Gambhir SS. Use of Positron Emission Tomography in Animal Research. ILAR J. 1. Januar 2001;42(3):219–32.

54. Abdulla S. PET imaging - Radiology Cafe [Internet]. 2017 [zitiert 29. März 2025]. Verfügbar unter: https://www.radiologycafe.com/frcr-physics-notes/molecular-imaging/pet-imaging/

55. Surti S. Update on time-of-flight PET imaging. J Nucl Med Off Publ Soc Nucl Med. Januar 2015;56(1):98–105.

56. Schlyer DJ. PET tracers and radiochemistry. Ann Acad Med Singapore. März 2004;33(2):146–54.

57. Van Dort ME, Rehemtulla A, Ross BD. PET and SPECT Imaging of Tumor Biology: New Approaches towards Oncology Drug Discovery and Development. Curr Comput Aided Drug Des. 2008;4(1):46–53.

58. Taddei C, Pike VW. [11C]Carbon monoxide: advances in production and application to PET radiotracer development over the past 15 years. EJNMMI Radiopharm Chem. 18. September 2019;4(1):25.

59. Mannheim JG, Schmid AM, Schwenck J, Katiyar P, Herfert K, Pichler BJ, u. a. PET/MRI Hybrid Systems. Semin Nucl Med. Juli 2018;48(4):332–47.

60. Kinahan PE, Townsend DW, Beyer T, Sashin D. Attenuation correction for a combined 3D PET/CT scanner. Med Phys. Oktober 1998;25(10):2046–53.

61. Watson CC, Casey ME, Michel C, Bendriem B. Advances in scatter correction for 3D PET/CT. In: IEEE Symposium Conference Record Nuclear Science 2004 [Internet]. Rome, Italy: IEEE; 2004 [zitiert 29. März 2025]. S. 3008–12. Verfügbar unter: http://ieeexplore.ieee.org/document/1466317/

62. Chun SY. The Use of Anatomical Information for Molecular Image Reconstruction Algorithms: Attenuation/Scatter Correction, Motion Compensation, and Noise Reduction. Nucl Med Mol Imaging. März 2016;50(1):13–23.

63. Killoran JH, Gerbaudo VH, Mamede M, Ionascu D, Park SJ, Berbeco R. Motion artifacts occurring at the lung/diaphragm interface using 4D CT attenuation correction of 4D PET scans. J Appl Clin Med Phys. 15. November 2011;12(4):3502.

64. Chen Y, An H. Attenuation Correction of PET/MR Imaging. Magn Reson Imaging Clin N Am. Mai 2017;25(2):245–55.

65. Lucignani G. SUV and segmentation: pressing challenges in tumour assessment and treatment. Eur J Nucl Med Mol Imaging. April 2009;36(4):715–20.

66. Benz MR, Evilevitch V, Allen-Auerbach MS, Eilber FC, Phelps ME, Czernin J, u. a. Treatment monitoring by 18F-FDG PET/CT in patients with sarcomas: interobserver variability of quantitative parameters in treatment-induced changes in histopathologically responding and nonresponding tumors. J Nucl Med Off Publ Soc Nucl Med. Juli 2008;49(7):1038–46.

67. Vettermann FJ, Diekmann C, Weidner L, Unterrainer M, Suchorska B, Ruf V, u. a. L-type amino acid transporter (LAT) 1 expression in 18F-FET-negative gliomas. EJNMMI Res. 14. Dezember 2021;11(1):124.

68. Zhang J, Xu Y, Li D, Fu L, Zhang X, Bao Y, u. a. Review of the Correlation of LAT1 With Diseases: Mechanism and Treatment. Front Chem. 20. Oktober 2020;8:564809.

69. Kobayashi K, Ohnishi A, Promsuk J, Shimizu S, Kanai Y, Shiokawa Y, u. a. ENHANCED TUMOR GROWTH ELICITED BY L-TYPE AMINO ACID TRANSPORTER 1 IN HUMAN MALIGNANT GLIOMA CELLS. Neurosurgery. Februar 2008;62(2):493–504.

70. Haining Z, Kawai N, Miyake K, Okada M, Okubo S, Zhang X, u. a. Relation of LAT1/4F2hc expression with pathological grade, proliferation and angiogenesis in human gliomas. BMC Clin Pathol. 28. Februar 2012;12:4.

71. Sharma R, D'Souza M, Jaimini A, Hazari PP, Saw S, Pandey S, u. a. A comparison study of (11)C-methionine and (18)F-fluorodeoxyglucose positron emission tomography-computed tomography scans in evaluation of patients with recurrent brain tumors. Indian J Nucl Med IJNM Off J Soc Nucl Med India. 2016;31(2):93–102.

72. Galldiks N, Unterrainer M, Judov N, Stoffels G, Rapp M, Lohmann P, u. a. Photopenic defects on O-(2-[18F]-fluoroethyl)-L-tyrosine PET: clinical relevance in glioma patients. Neuro-Oncol. 9. Oktober 2019;21(10):1331–8.

73. Katsanos AH, Alexiou GA, Fotopoulos AD, Jabbour P, Kyritsis AP, Sioka C. Performance of 18F-FDG, 11C-Methionine, and 18F-FET PET for Glioma Grading: A Meta-analysis. Clin Nucl Med. November 2019;44(11):864–9.

74. Grosu AL, Astner ST, Riedel E, Nieder C, Wiedenmann N, Heinemann F, u. a. An interindividual comparison of O-(2-[18F]fluoroethyl)-L-tyrosine (FET)- and L-[methyl-11C]methionine (MET)-PET in patients with brain gliomas and metastases. Int J Radiat Oncol Biol Phys. 15. November 2011;81(4):1049–58.

75. Habermeier A, Graf J, Sandhöfer BF, Boissel JP, Roesch F, Closs EI. System L amino acid transporter LAT1 accumulates O-(2-fluoroethyl)-L-tyrosine (FET). Amino Acids. Februar 2015;47(2):335–44.

76. Albert NL, Galldiks N, Ellingson BM, van den Bent MJ, Chang SM, Cicone F, u. a. PET-based response assessment criteria for diffuse gliomas (PET RANO 1.0): a report of the RANO group. Lancet Oncol. Januar 2024;25(1):e29–41.

77. Law I, Albert NL, Arbizu J, Boellaard R, Drzezga A, Galldiks N, u. a. Joint EANM/EANO/RANO practice guidelines/SNMMI procedure standards for imaging of gliomas using PET with radiolabelled amino acids and [18F]FDG: version 1.0. Eur J Nucl Med Mol Imaging. März 2019;46(3):540–57.

78. Bashir A, Mathilde Jacobsen S, Mølby Henriksen O, Broholm H, Urup T, Grunnet K, u. a. Recurrent glioblastoma versus late posttreatment changes: diagnostic accuracy of O-(2-[18F]fluoroethyl)-L-tyrosine positron emission tomography (18F-FET PET). Neuro-Oncol. 17. Dezember 2019;21(12):1595–606.

79. Brandsma D, Stalpers L, Taal W, Sminia P, Van Den Bent MJ. Clinical features, mechanisms, and management of pseudoprogression in malignant gliomas. Lancet Oncol. Mai 2008;9(5):453–61.

80. Jacobs F, Thierens H, Piepsz A, Bacher K, Van de Wiele C, Ham H, u. a. Optimised tracer-dependent dosage cards to obtain weight-independent effective doses. Eur J Nucl Med Mol Imaging. Mai 2005;32(5):581–8.

81. Lohmann P, Herzog H, Rota Kops E, Stoffels G, Judov N, Filss C, u. a. Dual-time-point O-(2-[(18)F]fluoroethyl)-L-tyrosine PET for grading of cerebral gliomas. Eur Radiol. Oktober 2015;25(10):3017–24.

82. Unterrainer M, Vettermann F, Brendel M, Holzgreve A, Lifschitz M, Zähringer M, u. a. Towards standardization of 18F-FET PET imaging: do we need a consistent method of background activity assessment? EJNMMI Res. Dezember 2017;7(1):48.

83. Lohmann P, Lerche C, Bauer EK, Steger J, Stoffels G, Blau T, u. a. Predicting IDH genotype in gliomas using FET PET radiomics. Sci Rep. 6. September 2018;8(1):13328.

84. Mittlmeier LM, Suchorska B, Ruf V, Holzgreve A, Brendel M, Herms J, u. a. 18F-FET PET Uptake Characteristics of Long-Term IDH-Wildtype Diffuse Glioma Survivors. Cancers. 24. Juni 2021;13(13):3163.

85. Lohmann P, Elahmadawy MA, Gutsche R, Werner JM, Bauer EK, Ceccon G, u. a. FET PET Radiomics for Differentiating Pseudoprogression from Early Tumor Progression in Glioma Patients Post-Chemoradiation. Cancers. 18. Dezember 2020;12(12):3835.

86. Sanghvi D. Post-treatment imaging of high-grade gliomas. Indian J Radiol Imaging. 2015;25(2):102–8.

87. Galldiks N, Stoffels G, Filss C, Rapp M, Blau T, Tscherpel C, u. a. The use of dynamic O-(2-18F-fluoroethyl)-L-tyrosine PET in the diagnosis of patients with progressive and recurrent glioma. Neuro-Oncol. 24. Mai 2015;nov088.

88. Kebir S, Fimmers R, Galldiks N, Schäfer N, Mack F, Schaub C, u. a. Late Pseudoprogression in Glioblastoma: Diagnostic Value of Dynamic O-(2-[18F]fluoroethyl)-L-Tyrosine PET. Clin Cancer Res. 1. Mai 2016;22(9):2190–6.

89. Verger A, Filss CP, Lohmann P, Stoffels G, Sabel M, Wittsack HJ, u. a. Comparison of O-(2- 18 F-Fluoroethyl)-L-Tyrosine Positron Emission Tomography and Perfusion-Weighted Magnetic Resonance Imaging in the Diagnosis of Patients with Progressive and Recurrent Glioma: A Hybrid Positron Emission Tomography/Magnetic Resonance Study. World Neurosurg. Mai 2018;113:e727–37.

90. Vettermann F, Suchorska B, Unterrainer M, Nelwan D, Forbrig R, Ruf V, u. a. Non-invasive prediction of IDH-wildtype genotype in gliomas using dynamic 18F-FET PET. Eur J Nucl Med Mol Imaging. November 2019;46(12):2581–9.

91. Zhou W, Huang Q, Wen J, Li M, Zhu Y, Liu Y, u. a. Integrated CT Radiomics Features Could Enhance the Efficacy of 18F-FET PET for Non-Invasive Isocitrate Dehydrogenase Genotype Prediction in Adult Untreated Gliomas: A Retrospective Cohort Study. Front Oncol. 2021;11:772703.

92. Li Z, Kaiser L, Holzgreve A, Ruf VC, Suchorska B, Wenter V, u. a. Prediction of TERTp-mutation status in IDH-wildtype high-grade gliomas using pre-treatment dynamic [18F]FET PET radiomics. Eur J Nucl Med Mol Imaging. Dezember 2021;48(13):4415–25.